



2303m2 CP

MEMORANDUM FOR PRS (In-House Publication)

FROM: PROI (STINFO)

06 March 2002

SUBJECT: Authorization for Release of Technical Information, Control Number: **AFRL-PR-ED-TP-2002-048**  
Karl Christe et al. (PRSP), "Synthesis and Characterization of the  $\text{SO}_2\text{N}_3^-$ ,  $(\text{SO}_2)_2\text{N}_3^-$  and  $\text{SO}_3\text{N}_3^-$   
Anions"

**Journal: (2002) Inorganic Chemistry**  
**(Deadline: N/A)**

**(Statement A)**

1. This request has been reviewed by the Foreign Disclosure Office for: a.) appropriateness of distribution statement, b.) military/national critical technology, c.) export controls or distribution restrictions, d.) appropriateness for release to a foreign nation, and e.) technical sensitivity and/or economic sensitivity.

Comments: \_\_\_\_\_  
\_\_\_\_\_  
\_\_\_\_\_

Signature \_\_\_\_\_

Date \_\_\_\_\_

2. This request has been reviewed by the Public Affairs Office for: a.) appropriateness for public release and/or b.) possible higher headquarters review.

Comments: \_\_\_\_\_  
\_\_\_\_\_  
\_\_\_\_\_

Signature \_\_\_\_\_

Date \_\_\_\_\_

3. This request has been reviewed by the STINFO for: a.) changes if approved as amended, b.) appropriateness of references, if applicable; and c.) format and completion of meeting clearance form if required

Comments: \_\_\_\_\_  
\_\_\_\_\_  
\_\_\_\_\_

Signature \_\_\_\_\_

Date \_\_\_\_\_

4. This request has been reviewed by PR for: a.) technical accuracy, b.) appropriateness for audience, c.) appropriateness of distribution statement, d.) technical sensitivity and economic sensitivity, e.) military/national critical technology, and f.) data rights and patentability

Comments: \_\_\_\_\_  
\_\_\_\_\_

APPROVED/APPROVED AS AMENDED/DISAPPROVED

PHILIP A. KESSEL

Date

Technical Advisor

Space and Missile Propulsion Division

## Synthesis and Characterization of the $\text{SO}_2\text{N}_3^-$ , $(\text{SO}_2)_2\text{N}_3^-$ , and $\text{SO}_3\text{N}_3^-$ Anions<sup>□</sup>

Karl O. Christe,<sup>\*†‡</sup> Jerry A. Boatz,<sup>†</sup> Michael Gerken,<sup>‡</sup> Ralf Haiges,<sup>‡</sup> Stefan Schneider,<sup>‡</sup>  
Thorsten Schroer,<sup>‡</sup> Fook S. Tham,<sup>§</sup> Ashwani Vij,<sup>†</sup> Vandana Vij,<sup>†</sup> Ross I. Wagner,<sup>‡</sup> and  
William W. Wilson<sup>†</sup>

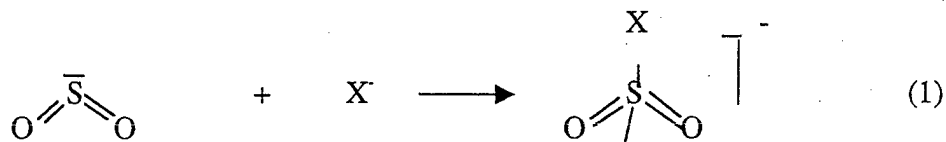
*Contribution from the Propulsion Sciences and Advanced Concepts Division, Air Force  
Research Laboratory (AFRL/PRS), Edwards AFB, California 93524, Loker Hydrocarbon  
Research Institute and Department of Chemistry, University of Southern California, Los Angeles,  
California 90089, University of California, Riverside, California 92521*

**Abstract:**  $\text{SO}_2$  solutions of azide anions are bright yellow and their Raman spectra indicate the presence of covalently bound azide. Removal of the solvent at  $-64^\circ\text{C}$  from  $\text{CsN}_3$  or  $\text{N}(\text{CH}_3)_4\text{N}_3$  solutions produces yellow  $(\text{SO}_2)_2\text{N}_3^-$  salts. Above  $-64^\circ\text{C}$ , these salts lose one mole of  $\text{SO}_2$ , resulting in white  $\text{SO}_2\text{N}_3^-$  salts that are marginally stable at room temperature and thermally decompose to the corresponding azides and  $\text{SO}_2$ . These anions were characterized by vibrational and  $^{14}\text{N}$  NMR spectroscopy, and theoretical calculations. Slow loss of the solvent by diffusion through the walls of a sealed Teflon tube containing a sample of  $\text{CsSO}_2\text{N}_3$  in  $\text{SO}_2$  resulted in white and yellowish single crystals that were identified by x-ray diffraction as  $\text{CsSO}_2\text{N}_3 \cdot \text{CsSO}_3\text{N}_3$  and  $\text{Cs}_2\text{S}_2\text{O}_5 \cdot \text{Cs}_2\text{S}_2\text{O}_7 \cdot \text{SO}_2$ , respectively. Pure  $\text{CsSO}_3\text{N}_3$  was also prepared and characterized by vibrational spectroscopy. The S-N bond in  $\text{SO}_2\text{N}_3^-$  is much weaker than that in  $\text{SO}_3\text{N}_3^-$ , resulting in decreased thermal stability, an increase in the S-N bond distance by  $0.23 \text{ \AA}$ , and an increased tendency to undergo rotational disorder. This marked difference is due to  $\text{SO}_3$  being a much stronger Lewis acid (pF value of 7.83) than  $\text{SO}_2$  (pF value of 3.99), thus forming a stronger S-N bond with the Lewis base  $\text{N}_3^-$ . The geometry of the free gaseous  $\text{SO}_2\text{N}_3^-$  anion was calculated at

the RHF, MP2, B3LYP, and CCSD(T) levels. The results show that only the correlated methods correctly reproduce the experimentally observed orientation of the SO<sub>2</sub> group.

## Introduction

Sulfur dioxide is a very interesting molecule. It serves not only as a very useful inorganic solvent, but also exhibits a rich reaction-chemistry. In addition to being a ligand with at least 9 different bonding modes,<sup>1</sup> it is also amphoteric and can act either as an electron donor (Lewis base) or acceptor (Lewis acid) molecule. As a donor, it can coordinate through its free valence electron pairs on either sulfur or oxygen. A typical example for the latter case is the oxygen-bridged adduct between SbF<sub>5</sub> and SO<sub>2</sub>.<sup>2</sup> As an acceptor, SO<sub>2</sub> likes to expand its coordination number around sulfur from three to four. Typical examples for compounds in which SO<sub>2</sub> acts as an acceptor are the SO<sub>2</sub>X<sup>-</sup> anions, where X<sup>-</sup> stands for a halide or pseudo-halide ion.<sup>3</sup>



During reactions, aimed at the metathetical synthesis of N<sub>5</sub><sup>+</sup>N<sub>3</sub><sup>-</sup>, the yellow color of the solutions of colorless N<sub>3</sub><sup>-</sup> in colorless SO<sub>2</sub> raised our curiosity. This is in marked contrast to solutions of N<sub>3</sub><sup>-</sup> in other polar solvents, such as water, that are colorless. Therefore, the SO<sub>2</sub>/N<sub>3</sub><sup>-</sup> system was studied in more detail. The results from this study were presented at the 13<sup>th</sup> European Symposium on Fluorine Chemistry<sup>4</sup> and a full account of this work is given in this paper. Our original report<sup>4</sup> provided the first evidence for the existence of the azidosulfite anion and was recently confirmed by an independent crystal structure determination of [N(CH<sub>3</sub>)<sub>4</sub>]<sup>+</sup>[SO<sub>2</sub>N<sub>3</sub>]<sup>-</sup>.<sup>5</sup> In spite of many known sulfur-nitrogen compounds,<sup>1</sup> including sulfuryl diazide<sup>6</sup> and azidosulfates,<sup>7-12</sup> no other reports on azidosulfites were found in the literature.

The  $\text{SO}_3\text{N}_3^-$  anion has previously been prepared by (a) the direct reaction between  $\text{SO}_3$  and  $\text{NaN}_3$ ;<sup>8</sup> (b) the reaction of  $\text{H}_2\text{NNHSO}_3\text{H}$  and  $\text{KNO}_2$ ;<sup>7</sup> (c) the reaction of  $[\text{Na}][\text{SO}_3\text{Cl}]$  and  $\text{N}_3^-$ ;<sup>9,12</sup> and (d) the reaction of  $\text{S}_2\text{O}_6\text{N}_3^-$  with  $\text{KOH/NaOH}$ .<sup>10</sup> Despite this diversity of synthetic routes, the  $\text{SO}_3\text{N}_3^-$  anion had been characterized only by elemental analyses and infrared spectroscopy.

## Experimental Section

*Caution! Azides are highly endothermic and often can decompose explosively. They should be handled on a small scale with appropriate safety precautions.*

**Materials and Apparatus.** Reactions were carried out in either flamed-out Pyrex glass tubes or Teflon-FEP or -PFA ampoules that contained Teflon coated magnetic stirring bars and were closed by stainless steel or Teflon valves. Volatile materials were handled either on a stainless steel / Teflon-FEP vacuum line<sup>13</sup> or a Pyrex glass vacuum line equipped with grease-free Kontes glass-Teflon valves. Nonvolatile solids were handled in the dry nitrogen atmosphere of a glove box. Infrared spectra were recorded on either a Mattson Galaxy or Midac M Series FT-IR spectrometer using dry powders pressed between  $\text{AgCl}$  windows in an Econo press (Barnes Engineering Co.). Raman spectra were recorded on either a Bruker Equinox 55 FT-RA spectrometer using a Nd-Yag laser at 1064 nm and Pyrex melting point capillaries, glass NMR or 9 mm Teflon-FEP tubes as sample containers or a Cary Model 83 spectrometer using the 488 nm exciting line of an Ar ion laser. NMR spectra were recorded on a Bruker Avance 400 FT-NMR spectrometer.

The  $\text{N}(\text{CH}_3)_4^+\text{N}_3^-$ ,<sup>14</sup>  $\text{CsN}_3$ ,<sup>15</sup> and  $\text{CsSO}_3\text{Cl}$ <sup>16</sup> starting materials were prepared by literature methods. The  $\text{SO}_2$  (Air Products, anhydrous grade, 99.9%) was dried over  $\text{CaH}_2$ . Trimethylsilyl azide (Aldrich, 95%) was condensed from a storage vessel at  $-35^\circ\text{C}$  into the reaction vessel at  $-196^\circ\text{C}$ .

**Preparation of  $M^+SO_2N_3^-$  [ $M = Cs$  or  $N(CH_3)_4$ ].** In a typical experiment, a 5 mm Pyrex glass NMR tube, closed by a concentric, grease-free Teflon valve (Wilmad Glass Co.) was loaded with  $CsN_3$  (1.335 mmol) in the glove box. The tube was attached to the Pyrex vacuum line and evacuated; then anhydrous  $SO_2$  (0.765 mL) was condensed into the tube at  $-196^\circ C$ . The mixture was warmed to room temperature, and the  $CsN_3$  dissolved giving a yellow solution. In the presence of traces of moisture, a small amount of a white precipitate formed that was identified by its infrared and Raman spectra as  $Cs_2S_2O_5$ .<sup>17</sup> The tube and its contents were cooled to  $-22^\circ C$ , and the  $SO_2$  solvent was pumped off in a dynamic vacuum, leaving behind a white solid (322.0 mg, weight calculated for 1.335 mmol of  $CsSO_2N_3 = 319.1$  mg).

**Preparation of  $M^+(SO_2)_2N_3^-$  [ $M = Cs$  or  $N(CH_3)_4$ ].** In a manner similar to that used for the preparation of  $CsSO_2N_3$ ,  $CsN_3$  (1.346 mmol) was loaded into a Pyrex NMR tube equipped with a glass-Teflon valve, and anhydrous  $SO_2$  (0.769 mL) was added in vacuo to the tube at  $-196^\circ C$ . After warming to room temperature to dissolve all the  $CsN_3$ , the tube was cooled to  $-64^\circ C$ , and the  $SO_2$  was removed slowly in a dynamic vacuum for 4 hours. The nonvolatile residue consisted of a yellow solid (406 mg, weight calculated for 1.346 mmol of  $Cs(SO_2)_2N_3 = 407.9$  mg).

**Preparation of  $[Cs][SO_3N_3]$ .** Inside a dry box, a glass vessel, equipped with a Kontes glass-Teflon valve and a Teflon-coated stirring bar, was loaded with  $[Cs][SO_3Cl]$  (2.383 mmol). On a glass vacuum line,  $(CH_3)_3SiN_3$  (8.940 mmol) was distilled onto the solid at  $-196^\circ C$  and allowed to warm to room temperature. After stirring the suspension for two days, volatiles were removed at room temperature yielding a white solid. Raman spectroscopic characterization of the solid revealed the presence of  $[Cs][SO_3Cl]$  and  $[Cs][SO_3N_3]$ . Four additional cycles of adding fresh  $(CH_3)_3SiN_3$ , followed by removal of all volatiles at room temperature while monitoring the

progress of the reaction by Raman spectroscopy, resulted in a quantitative yield of pure  $[\text{Cs}][\text{SO}_3\text{N}_3]$ .

**Crystal Structure Determination of  $\text{CsSO}_2\text{N}_3 \cdot \text{CsSO}_3\text{N}_3$ .** About 0.5 mL of  $\text{SO}_2$  was condensed onto anhydrous  $\text{CsN}_3$  in a 4 mm FEP NMR tube that was then evacuated at  $-196^\circ\text{C}$  and heat-sealed. The yellowish solution was allowed to stand for several weeks during which time  $\text{SO}_2$  diffused slowly through the walls of the tube, and a mixture of diffraction-quality, prismatic, clear, colorless (compound 1,  $\text{CsSO}_2\text{N}_3 \cdot \text{CsSO}_3\text{N}_3$ ) and pale yellow (compound 2,  $\text{Cs}_2\text{S}_2\text{O}_5 \cdot \text{Cs}_2\text{S}_2\text{O}_7 \cdot \text{SO}_2$ ) crystals was formed. The FEP tube was then cut open under a stream of cold  $\text{N}_2$  gas at  $\sim -80^\circ\text{C}$ , and the crystalline contents were dropped into the lip of a low-temperature crystal-mounting apparatus. A Nylon Cryoloop, attached to a magnetic base, was used to trap a crystal, using PFPE (perfluoropolyether) oil, and to mount it on the magnetic goniometer. The single crystal diffraction data were collected on a Bruker 3-circle platform diffractometer, equipped with a SMART<sup>18</sup> CCD (charge coupled device) detector with the  $\chi$ -axis fixed at  $54.74^\circ$ , and using  $\text{MoK}_\alpha$  radiation ( $\lambda = 0.71073 \text{ \AA}$ ) from a fine-focus tube. This diffractometer was equipped with an LT-3 apparatus for low-temperature data collection using controlled liquid nitrogen boil off. Cell constants were determined from 90 thirty-second frames at  $-100^\circ\text{C}$  (1) or at  $-70^\circ\text{C}$  (2). A complete hemisphere of data was collected, using 1271 frames at 30 s/frame at a detector resolution of  $512 \times 512$  pixels, including 50 frames that were collected at the beginning and end of the data collection to monitor crystal decay. The frames were then processed on a PC running on Windows NT software by using the SAINT software<sup>19</sup> to give the hkl file corrected for  $L_p$ /decay. The absorption correction was performed using the SADABS<sup>20</sup> program. The structures were solved by the direct method, using the SHELX-97 program,<sup>21</sup> and refined by the least squares method on  $F^2$ , SHELXL-97,<sup>22</sup> incorporated in SHELXTL Suite 5.10

for Windows NT.<sup>23</sup> All atoms were refined anisotropically. For the anisotropic displacement parameters, the  $U(eq)$  is defined as one third of the trace of the orthogonalized  $U_{ij}$  tensor.

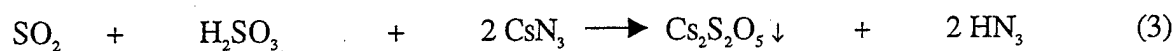
**Theoretical Calculations.** Theoretical calculations were carried out on IBM RS/6000 work stations using the GAMESS,<sup>24</sup> Gaussian 98,<sup>25</sup> and ACES II<sup>26</sup> program systems and the restricted Hartree Fock (RHF),<sup>27</sup> the density functional B3LYP,<sup>28</sup> and the correlated MP2<sup>29</sup> and single- and double-excitation coupled cluster methods,<sup>30</sup> including a non-iterative treatment of connected triple excitations.<sup>31</sup>

## Results and Discussion

**The  $SO_2/N_3^-$  System.** In common solvents, such as water, the  $N_3^-$  anion dissolves without color and retains its centro-symmetric, linear  $D_{\infty h}$  structure, as shown by its spectroscopic properties. For example, an aqueous  $NaN_3$  solution exhibits in the Raman spectrum only the symmetric  $N_3^-$  stretching mode at  $1340\text{ cm}^{-1}$  and in the  $^{14}\text{N}$  NMR spectrum two resonances at  $-282.2$  and  $-133.5$  ppm, respectively, with an area ratio of 2:1. By contrast, a solution of  $CsN_3$  in liquid  $SO_2$  is intense yellow, exhibits a strong Raman band at  $2016\text{ cm}^{-1}$ , and its  $^{14}\text{N}$  resonance for the two terminal nitrogen atoms is deshielded by 80 ppm relative to that of the free ion (Table 1). The  $^{14}\text{N}$  NMR spectrum of a 1:1 mixture of  $CsN_3$  and  $SO_2$  in  $CH_3NO_2$  solution exhibits also two resonances at  $\delta = -209.9$  and  $-132.5$  ppm, respectively, with an area ratio of 2:1. These chemical shifts are similar to those of  $-201.7$  and  $-133.9$  ppm observed for the  $SO_2$  solution. The observation of a single resonance for the terminal nitrogen atoms, even for solutions of the 1:1 and 1:2 adducts in  $CH_3CN$  at low temperatures, and the weak temperature dependence of the chemical shifts indicate that the  $SO_2$  groups in azidosulfites undergo rapid exchange on the NMR time scale.

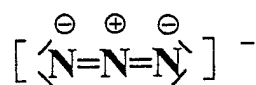


These observations are strong indications that  $\text{SO}_2$  forms adducts with the azide anion. The combining ratios of  $\text{N}_3^-$  with  $\text{SO}_2$  were studied both experimentally and by theoretical calculations. It was found that at  $-64^\circ\text{C}$   $\text{SO}_2$  forms with  $\text{Cs}^+\text{N}_3^-$  yellow 2:1 adducts that lose at about  $-30^\circ\text{C}$  one mole of  $\text{SO}_2$  and yield white 1:1 adducts. The 1:1 adducts are marginally stable at room temperature and, when heated to about  $60^\circ\text{C}$ , decompose to pure  $\text{N}_3^-$  and  $\text{SO}_2$ . The corresponding  $\text{N}(\text{CH}_3)_4^+$  salts are thermally somewhat less stable. The underlying chemistry can be used for the conversion of insoluble halides, such as fluoride, into azide. For example,  $\text{CsF}$  is insoluble in most organic solvents and reacts only incompletely with reagents such as trimethylsilylazide. It reacts, however, with  $\text{SO}_2$  forming soluble  $\text{SO}_2\text{F}^-$ . The fluoride in  $\text{SO}_2\text{F}^-$  can then readily be exchanged for azide using trimethylsilylazide, resulting in the formation of  $\text{SO}_2\text{N}_3^-$ . The latter is then thermally decomposed to give pure azide and  $\text{SO}_2$ .<sup>15</sup> During the pyrolysis of  $\text{SO}_2\text{N}_3^-$ , no evidence was obtained for any  $\text{N}_2$  elimination before the loss of all the  $\text{SO}_2$  which might have offered a potential synthesis for  $\text{NSO}_2^-$  salts.<sup>32-34</sup> In the presence of small amounts of moisture, colorless cesium salts of  $\text{S}_2\text{O}_5^{2-}$  and  $\text{S}_2\text{O}_7^{2-}$  can be formed as insoluble by-products.<sup>35</sup>



As  $\text{SO}_2$  has very little vapor pressure below  $-64^\circ\text{C}$ , the isolation of well defined adducts containing more than two  $\text{SO}_2$  molecules per  $\text{N}_3^-$  could not be studied experimentally.

In agreement with the experimental observations, the theoretical calculations show that  $\text{SO}_2$  can form stable 1:1 and 2:1 adducts with  $\text{N}_3^-$ . In the 1:1 adduct, the  $\text{SO}_2$  molecule is attached to one of the terminal nitrogens of the azide anion. This is in accord with the negative charges in  $\text{N}_3^-$  residing mainly on the terminal nitrogen atoms, thus making them the better donors.



The N-S bond of the resulting adducts is relatively long, varies strongly with the computational level, and ranges for the 1:1 adduct from 1.91 Å at the RHF level to 2.36 Å at the MP2 level.

For the 2:1 adducts, the two SO<sub>2</sub> groups could reside on either the same or both terminal nitrogen atoms. The energy differences between the 1,1 adduct (rN-S = 2.47 Å at MP2) and the 1,3 adduct (rN-S = 2.56 Å) are predicted to be small, i.e., less than 1 kcal/mol at the MP2 and less than 4 kcal/mol at the B3LYP level of theory in favor of the 1,1 adduct.

Based on our calculations, the addition of a third SO<sub>2</sub> molecule to the 1,1 adduct lengthens the two original 1,1 N-S bonds to 2.52 Å, but the third N-S bond to the other terminal nitrogen is much weaker at 2.87 Å. Similarly, the addition of a fourth SO<sub>2</sub> molecule affects the three original N-S bonds relatively little; the two geminal N-S bonds at 2.54 Å become slightly longer and the third N-S bond at 2.80 Å becomes slightly shorter; however, the fourth N-S bond at 3.19 Å becomes much longer. These calculations at the MP2 level confirm that in the presence of excess SO<sub>2</sub> the N-S bonds become very weak, thus accounting for the observed facile N-S bond breakage on an NMR timescale. A more detailed discussion of the calculated structures will be given below.

The SO<sub>2</sub>N<sub>3</sub><sup>-</sup> anion can be described as either a donor-acceptor adduct between the Lewis acid SO<sub>2</sub> and the Lewis base N<sub>3</sub><sup>-</sup> or, by analogy to many known SO<sub>2</sub>X<sup>-</sup> (X = halogen or pseudohalogen) anions, as an azidosulfite anion. Whereas either description is acceptable, the description of the higher (SO<sub>2</sub>)<sub>n</sub>N<sub>3</sub><sup>-</sup> adducts as azidopolysulfites is inappropriate because there is no significant interaction between the SO<sub>2</sub> ligands. For the analogous (SO<sub>3</sub>)<sub>n</sub>N<sub>3</sub><sup>-</sup> adducts, azidopolysulfate structures have previously been suggested;<sup>10</sup> however it appears likely that these SO<sub>3</sub> analogues also contain discrete SO<sub>3</sub> units and not polysulfate anions.

**Crystal structures of  $\text{CsSO}_2\text{N}_3$  and  $\text{CsSO}_3\text{N}_3$ .** The white crystals (compound 1), obtained from a sample of  $\text{CsSO}_2\text{N}_3$  in  $\text{SO}_2$  solution that was kept in a Teflon NMR tube at room temperature for several weeks, had the composition  $\text{CsSON}_3 \cdot \text{CsSO}_3\text{N}_3$ . These crystals were stable only at low-temperature or under an atmosphere of  $\text{SO}_2$  at room temperature. The asymmetric unit in the crystal lattice of 1 shows two Cs, two sulfur and five oxygen atoms besides six nitrogen atoms forming two azide groups (Figure 1 and Tables 2-4). The cesium and sulfur atoms, and O1 and N2 lie on special positions. The large thermal ellipsoids observed for the N1, N3, N4, N5 and N6 atoms indicate a disorder across the crystallographic mirror plane. These atoms were then moved off the mirror plane and refined which resulted in two disordered azide conformations on the sulfur groups. In  $\text{SO}_2\text{N}_3^-$ , the sulfur atom S2 is connected to three oxygen positions with a total occupancy of 2 and, therefore, is attributed to an  $\text{SO}_2$  group. The oxygen atoms on S2 exhibit rotational disorder and have refined occupancies for O3 and O5 of 64 and 36 %, respectively. A comparison of the geometry found in this study for  $\text{SO}_2\text{N}_3^-$  in its cesium salt (see Figure 2) with that in the ordered  $\text{N}(\text{CH}_3)_4^+$  salt<sup>5</sup> and the theoretical predictions at the correlated level (see Figure 3 and Table 4) shows good agreement and demonstrates that the counter ion does not strongly influence the structure of  $\text{SO}_2\text{N}_3^-$ .

The  $\text{SO}_3\text{N}_3^-$  anion is also slightly disordered. The N1 and N3 atoms are disordered across the crystallographic symmetry plane through S1, O1, and N2 (see Figure 4). Figure 5 depicts one of the two disordered components. Furthermore, the rotation of the  $\text{SO}_3$  group with respect to the  $\text{N}_3$  group deviates from the predictions at the MP2 and B3LYP levels of theory (see Table 5 and Figure 6). In the free gaseous anion, the O1, S1, N1, N2, and N3 atoms are all predicted to be coplanar, with O1 being *trans* to the azide group, while in the experimental solid-state structure it is *cis*. Since the calculated energy difference between the *cis*- and *trans*-rotamers is very small

due to the weak S-N bond and its low frequency ( $33\text{ cm}^{-1}$ ) torsion mode, the orientation of the  $\text{SO}_3$  group is easily affected by the strong oxygen-cesium interactions in the lattice (see below).

A comparison of the experimental structures of  $\text{SO}_2\text{N}_3^-$  and  $\text{SO}_3\text{N}_3^-$  shows a remarkable difference of  $0.23\text{ \AA}$  for the S-N distances, i. e.,  $1.981(12)\text{ \AA}$  for  $\text{SO}_2\text{N}_3^-$  and  $1.754(10)\text{ \AA}$  and  $\text{SO}_3\text{N}_3^-$ . The observed difference agrees well with that of  $0.32\text{ \AA}$  predicted at the B3LYP level and can be rationalized by the large difference in the Lewis acidities of  $\text{SO}_2$  and  $\text{SO}_3$ . Based on the Christie/Dixon pF scale,<sup>36</sup>  $\text{SO}_2$  and  $\text{SO}_3$  have pF values of 3.99 and 7.83, respectively. If one views the  $\text{SO}_2\text{N}_3^-$  and  $\text{SO}_3\text{N}_3^-$  anions as Lewis acid / Lewis base adducts (see above), it is not surprising that the stronger Lewis acid  $\text{SO}_3$  forms the more stable adduct with the azide anion. Due to its longer S-N bond, the  $\text{SO}_2\text{N}_3^-$  anion should undergo  $\text{SO}_n$  group rotation even more easily than  $\text{SO}_3\text{N}_3^-$ . Therefore, one can expect the orientations of the  $\text{SO}_n$  groups in the  $\text{SO}_n\text{N}_3^-$  anions to vary significantly from one salt to another. The  $\text{N}_\beta\text{-N}_\gamma$  distances at  $\sim 1.13\text{ \AA}$  are significantly shorter than the  $\text{N}_\alpha\text{-N}_\beta$  distances at  $\sim 1.21\text{ \AA}$  and are characteristic for covalent azides with significant triple and double bond character, respectively. With increasing S-N bond length and a weakening of the  $\text{SO}_2\text{-N}_3^-$  interaction, the  $\text{N}_\alpha\text{-N}_\beta$  and  $\text{N}_\beta\text{-N}_\gamma$  bonds become, as expected, more similar and their values approach those of the free  $\text{N}_3^-$  anion.

The  $\text{CsSO}_2\text{N}_3\cdot\text{CsSO}_3\text{N}_3$  structure exhibits many short contacts indicative of strong interionic interactions. Thus, all the  $\text{Cs}\cdots\text{O}$  distances fall within the range of  $3.047(6)$  ( $\text{Cs2}\cdots\text{O1}$ ) to  $3.40(2)$  ( $\text{Cs2}\cdots\text{O5}$ )  $\text{\AA}$  and are considerably shorter than the sum of their van der Waals radii of about  $4.5\text{ \AA}$ .<sup>37</sup> The  $\text{Cs}\cdots\text{N}$  contacts of  $3.219(13)$  and  $3.305(11)\text{ \AA}$ , involving the  $\text{SO}_2\text{N}_3^-$  and the  $\text{SO}_3\text{N}_3^-$  groups, respectively, are also significantly shorter than the sum of their van der Waals radii of about  $4.54\text{ \AA}$ . The  $\text{S1}\cdots\text{Cs2}$  contact of  $3.848(2)\text{ \AA}$  is also considerably shorter than the average distance of  $\sim 4.43\text{ \AA}$  for the remaining  $\text{Cs}\cdots\text{S}$  contacts.

The short Cs...O contacts mentioned above result in a three-dimensional network of four-membered  $\text{Cs}_2\text{O}_2$  rings involving alternating  $\text{SO}_3\text{N}_3$  and  $\text{SO}_2\text{N}_3$  units (Figure 1). A mean least square plane analysis of these two four-membered rings shows that they are twisted by  $93.4^\circ$  with respect to each other. The cesium-sulfur network (Figure 7) forms the basic crystal lattice that is built up of face- and edge-sharing cuboids stacked in a stair-like fashion.

The yellow impurity **2** was identified as a double salt of  $\text{Cs}_2\text{S}_2\text{O}_5$  and  $\text{Cs}_2\text{S}_2\text{O}_7$  with a molecule of  $\text{SO}_2$  present as a solvate. The crystal structures of the separate anions have previously been reported,<sup>38-41</sup> and the structure of this ternary compound will be discussed in a forthcoming paper.

**Vibrational Spectra and Theoretical Calculations.** The vibrational spectra of  $\text{CsSO}_2\text{N}_3$ ,  $\text{N}(\text{CH}_3)_4\text{SO}_2\text{N}_3$ ,  $\text{Cs}(\text{SO}_2)_2\text{N}_3$ ,  $\text{N}(\text{CH}_3)_4(\text{SO}_2)_2\text{N}_3$ , and  $\text{CsSO}_3\text{N}_3$  are summarized in Tables 6-8 and Figures 8-11. The assignments were made by comparison with the calculated spectra and are supported by normal coordinated analyses. The correctness of the given mode descriptions was established by the calculated potential energy distributions. All the listed calculations were carried out with a 6-311+G(d) basis set. The calculations at the B3LYP level were also done with 6-311+G(2d) and aug-cc-pvtz basis sets and showed that the choice of the basis set had little influence on the results. For the ease of presentation, the spectra are discussed in the following order:  $\text{SO}_2\text{N}_3^-$ ,  $(\text{SO}_2)_2\text{N}_3^-$ ,  $\text{N}_3^-$  in  $\text{SO}_2$  solution, and  $\text{SO}_3\text{N}_3^-$ .

**$\text{SO}_2\text{N}_3^-$ .** The structure of the  $\text{SO}_2\text{N}_3^-$  anion is well established by the crystal structures of its  $\text{N}(\text{CH}_3)_4^{+5}$  and  $\text{Cs}^+$  (Fig. 2) salts and the results from the theoretical calculations (Figure 3 and Table 4). It must be emphasized that only the calculations at a correlated level (Figure 3) duplicate the experimentally observed orientation of the  $\text{SO}_2$  group. At the RHF level, the  $\text{SO}_2$  group points in the same direction as the azido group (Fig. 12). However, the energy difference

between the structures of Figures 3 and 12 is only about one kcal/mol because of the rotational barrier along the N-S bond in  $\text{SO}_2\text{N}_3^-$  ( $\nu = 22 \text{ cm}^{-1}$  at the B3LYP level) being even lower than that in  $\text{SO}_3\text{N}_3^-$  ( $\nu = 33 \text{ cm}^{-1}$ ). The agreement between the observed and the calculated spectra (see Table 6) is satisfactory if one keeps in mind that the skeletal modes involving the very long N-S bonds are strongly correlation dependent. Thus, the uncorrelated RHF method underestimates the bond length of the S-N bond resulting in high frequency values for the modes involving the N-S bond. On the other hand, all the correlated methods significantly overestimate the S-N bond length (see Tables 4 and 5) resulting in low frequency values for these modes. If one assumes that the actual bond lengths and frequencies fall between the uncorrelated and the correlated values, the fit between calculated and observed data becomes satisfactory. These results, together with our previous study of the  $\text{SO}_2\text{F}^-$  anion,<sup>42</sup> demonstrate the difficulties associated with the accurate calculation of highly ionic, long bonds. In view of the significant discrepancies between the observed and calculated frequencies, the calculated force fields have not been included in this paper.

$(\text{SO}_2)_2\text{N}_3^-$ . Whereas the structure of the  $\text{SO}_2\text{N}_3^-$  anion is firmly supported by its crystal structures, only Raman data are available for the  $(\text{SO}_2)_2\text{N}_3^-$  ion. Since the negative charges in  $\text{N}_3^-$  are located on the two terminal nitrogen atoms (see above), the  $\text{SO}_2$  groups must be attached to these. However, the two  $\text{SO}_2$  groups could be attached to the same or to different nitrogen atoms. Theoretical calculations at the B3LYP (Figures 13 and 15) and MP2 (Figures 14 and 16) levels of theory favor the geminal 1,1- $(\text{SO}_2)_2\text{N}_3^-$  over the terminal 1,3- $\text{O}_2\text{SNNNSO}_2^-$  adduct by 3.5 and 0.4 kcal/mol, respectively. Figures 13 and 14 also show that the B3LYP and MP2 calculations result in very different minimum energy structures for the 1,3-adduct. At the MP2 level there is, in addition to the  $\text{N}_\alpha\text{-S}$  bond with 2.56 Å, also significant  $\pi\text{-}\pi$  interaction between the  $\text{N}=\text{N}$  and

S=O double bonds resulting in an N<sub>p</sub>-O interaction of 2.84 Å, while at the B3LYP level the interaction occurs mainly through N-S bonds. Calculations were also carried out using the MP2 structure as the starting point for the B3LYP calculation and *vice versa*, but in each case the calculations reverted back to the structures shown in Figures 13 and 14, establishing that they are the true minima for each method. For the 1,1-adducts, the MP2 and B3LYP structures are more similar (Figures 15 and 16).

Distinction between the 1,1- and the 1,3- structures is possible from the observed Raman intensities (see Table 7). In the 1,3-structures the relative intensities of the antisymmetric and the symmetric azide stretching modes are comparable, while in the 1,1 adducts the antisymmetric stretching mode is much more intense than the symmetric one. Furthermore, in the 1,3 adduct many of the low-frequency skeletal modes are of low Raman intensity, while in the 1,1-adduct they are more intense and of comparable intensity. The observed spectra (see Table 7 and Figure 10) clearly favor the energetically favored 1,1-structure.

**SO<sub>2</sub> Solutions of N<sub>3</sub><sup>-</sup>.** The Raman spectra of the yellow solutions of N<sub>3</sub><sup>-</sup> in liquid SO<sub>2</sub> show bands at about 2016(s) (ν<sub>as</sub>N<sub>3</sub>), 1274(w) (ν<sub>as</sub>SO<sub>2</sub>), 1120(vs) (ν<sub>sym</sub>SO<sub>2</sub>), 646(mw) (δN<sub>3</sub>), 400(br), and 230(br) cm<sup>-1</sup> that are in accord with the spectra observed for the yellow, solid 1,1-(SO<sub>2</sub>)<sub>2</sub>N<sub>3</sub><sup>-</sup> adduct. In view of the similar spectra and the fact that the theoretical calculations indicate that the bonding of a third and fourth SO<sub>2</sub> ligand to (SO<sub>2</sub>)<sub>2</sub>N<sub>3</sub><sup>-</sup> becomes increasingly weaker (see above), the yellow species present in the N<sub>3</sub>/SO<sub>2</sub> solutions is attributed to the 1,1-(SO<sub>2</sub>)<sub>2</sub>N<sub>3</sub><sup>-</sup> anion.

**SO<sub>3</sub>N<sub>3</sub><sup>-</sup>.** The structure of this anion is firmly established by the x-ray diffraction results (Figures 4 and 5). The theoretical calculations at the MP2 and B3LYP levels (see Tables 5 and 8 and Figure 6) result in almost identical geometries, however, compared to the experimental

structure, the  $\text{SO}_3$  group is rotated by  $60^\circ$  about the S-N axis. As for  $\text{SO}_2\text{N}_3^-$ , both methods significantly overestimate the N-S bond length, in this case by  $0.12 \text{ \AA}$ . This bond distance overestimate results in an underestimate of those vibrational frequencies involving the S-N bond (see Table 8), but otherwise the agreement between observed and calculated spectra is satisfactory. The fact that the S-N bond in  $\text{SO}_3\text{N}_3^-$  is significantly shorter than that in  $\text{SO}_2\text{N}_3^-$  has already been explained above by the increased Lewis acidity of  $\text{SO}_3$ . This increased withdrawal of electron density and negative charge from the azide anion in  $\text{SO}_3\text{N}_3^-$  also causes a marked decrease in the N-N bond lengths, an increase in the average  $\text{N}_3$  stretching and bending frequencies, and an increased bond length difference between the  $\text{N}_\alpha\text{-N}_\beta$  and  $\text{N}_\beta\text{-N}_\gamma$  bonds.

**Conclusions.** The  $\text{N}_3^-$  anion acts as a pseudohalide and dissolves in liquid  $\text{SO}_2$  forming yellow donor-acceptor adducts containing at least two  $\text{SO}_2$  molecules per  $\text{N}_3^-$ . At low temperature, yellow  $(\text{SO}_2)_2\text{N}_3^-$  salts can be isolated in which both  $\text{SO}_2$  molecules are probably attached to the same terminal nitrogen atom. At about  $-30^\circ\text{C}$ , one mole of  $\text{SO}_2$  can be pumped off, resulting in marginally stable, colorless  $\text{SO}_2\text{N}_3^-$  salts that can be converted at about  $50^\circ\text{C}$  into pure azides. The azidosulfites are analogous to the previously known azidosulfates, but possess a significantly weaker S-N bond resulting in lowered thermal stability.

### Acknowledgements

The authors thank the National Science Foundation, the Defense Advanced Project Agency, and the Air Force Office of Scientific Research for financial support. S.S. thanks the Alexander von Humboldt Foundation for a Feodor-Lynen fellowship and M. G. the Natural Sciences and Engineering Research Council of Canada for a postdoctoral fellowship. This work was also supported in part by a grant of IBM SP time from the Aeronautical Systems Center at



Wright-Patterson Air Force Base, a Department of Defense High Performance Computing Major Shared Resource Center.

### Supporting Information Available

Tables of structure determination summary, atomic coordinates, bond lengths and angles and anisotropic displacement parameters of  $\text{CsSO}_2\text{N}_3$ ,  $\text{CsSO}_3\text{N}_3$  in CIF format. This material is available free of charge via the internet at <http://pubs.acs.org>.

### References

<sup>a</sup>This paper is dedicated to Professor Dieter Naumann on the occasion of his 60<sup>th</sup> birthday.

<sup>†</sup>Air Force Research Laboratory

<sup>‡</sup>University of Southern California

<sup>§</sup>UC Riverside

- (1) Greenwood, N. N.; Earnshaw, A. *Chemistry of the Elements*, Second Edition, Butterworth-Heinemann, Oxford, 1998, p. 721-746.
- (2) Bacon, J.; Dean, P. A. W.; Gillespie, R. J. *Can. J. Chem.* **1969**, *47*, 1655.
- (3) Kornath, A.; Blecher, O.; Ludwig, R. *J. Am. Chem. Soc.* **1999**, *121*, 4019, and references cited therein.

- (4) Vij, A.; Wilson, W.; Sheehy, J.; Boatz, J.; Gerken, M.; Schneider, S.; Schroer, T.; Haiges, R.; Wagner, R.; Tham, F.; Christe, K.; Paper B7, presented at the 13<sup>th</sup> European Symposium on Fluorine Chemistry, Bordeaux, France, July 15-20, 2001.
- (5) Kornath, A.; Blecher, O.; Ludwig, R. *Z. Anorg. Allg. Chem.* **2002**, *628*, 183.
- (6) Curtius, T.; Schmidt, F. *Ber. Dtsch. Chem. Ges.* **1922**, *55*, 1571.
- (7) Traube, W.; Vockerodt, A. *Ber. Dtsch. Chem. Ges.* **1914**, *47*, 943.
- (8) Beck, G. *J. Prakt. Chem.* **1940**, *156*, 227.
- (9) Elsner, H.; Ratz, H. *German Patent* 886,298 **1953**.
- (10) Lehmann, H. A.; Holznagel, W. *Z. Anorg. Allg. Chem.* **1958**, *293*, 314.
- (11) Ruff, J. K. *Inorg. Chem.* **1965**, *4*, 567.
- (12) Shozda, R. J.; Vernon, J. A. *J. Org. Chem.* **1967**, *32*, 2876.
- (13) Christe, K. O.; Wilson, W. W.; Schack, C. J.; Wilson, R. D. *Inorg. Synth.* **1986**, *24*, 39.
- (14) Christe, K. O.; Wilson, W. W.; Bau, R.; Bunte, S. W. *J. Am. Chem. Soc.* **1992**, *114*, 3411.
- (15) Gerken, M.; Schneider, S.; Schroer, T.; Christe, K. O. *Z. Anorg. Allg. Chem.* in press.
- (16) Ciruna, J. A.; Robinson, E. A. *Can. J. Chem.* **1968**, *46*, 1715.
- (17) Siebert, H. *Anwendungen der Schwingungsspektroskopie in der Anorganischen Chemie, Anorganische und Allgemeine Chemie in Einzeldarstellungen, VII*; Springer Verlag: Berlin, 1966, p 102; Herlinger, A. W.; Long, T. V. *Inorg. Chem.* **1969**, *8*, 2661.
- (18) SMART V 4.045, Software for the CCD Detector System, Bruker AXS, Madison, WI, 1999.
- (19) SAINT V 4.035, Software for the CCD Detector System, Bruker AXS, Madison, WI, 1999.

- (20) SADABS, Program for absorption correction for area detectors, Version 2.01, Bruker AXS, Madison, WI (2000).
- (21) Sheldrick, G. M. SHELXS-97, Program for the Solution of Crystal Structure, University of Göttingen, Germany, 1997.
- (22) Sheldrick, G. M. SHELXL-97, Program for the Refinement of Crystal Structure, University of Göttingen, Germany, 1997.
- (23) SHELXTL 5.10 for Windows NT, Program library for Structure Solution and Molecular Graphics, Bruker AXS, Madison, WI (1997).
- (24) Schmidt, M.W.; Baldrige, K.K.; Boatz, J.A.; Elbert, S.T.; Gordon, M.S.; Jensen, J.H.; Koseki, S.; Matsunaga, N.; Nguyen, K.A.; Su, S.J.; Windus, T.L.; Dupuis, M.; Montgomery, J.A. *J. Comp. Chem.* **1993**, *14*, 1347-1363.
- (25) Frisch, M.J.; Trucks, G.W.; Schlegel, H.B.; Scuseria, G.E.; Robb, M.A.; Cheeseman, J.R.; Zakrzewski, V.G.; Montgomery, J.A., Jr.; Stratmann, R.E.; Burant, J.C.; Dapprich, S.; Millam, J.M.; Daniels, R.E.; Kudin, K.N.; Strain, M.C.; Farkas, O.; Tomasi, J.; Barone, V.; Cossi, M.; Cammi, R.; Mennucci, B.; Pomelli, C.; Adamo, C.; Clifford, S.; Ochterski, J.; Peterson, G.A.; Ayala, P.Y.; Cui, Q.; Morokuma, K.; Malick, D.K.; Rabuck, A.D.; Raghavachari, K.; Foresman, J.B.; Cioslowski, J.; Ortiz, J.V.; Stefanov, B.B.; Liu, G.; Liashenko, A.; Piskorz, P.; Komaromi, I.; Gomperts, R.; Martin, R. L.; Fox, D. J.; Keith, T.; Al-Laham, M. A.; Peng, C.Y.; Nanayakkara, A.; Gonzalez, C.; Challacombe, M.; Gill, P.M.W.; Johnson, B.; Chen, W.; Wong, M.W.; Andres, J.L.; Gonzalez, C.; Head-Gordon, M.; Replogle, E.S.; Pople, J.A. *Gaussian 98*, revision A.6; Gaussian, Inc.: Pittsburgh, PA, 1998.
- (26) Stanton, J.F.; Gauss, J.; Watts, J.D.; Nooijen, M.; Oliphant, N.; Perera, S.A.; Szalay, P.G.; Lauderdale, W.J.; Gwaltney, S.R.; Beck, S.; Balkova, A.; Bernholdt, D.E.; Baeck,

- K.K.; Rozyczko, P.; Sekino, H.; Hober, C.; Bartlett, R.J. *ACES II, Quantum Theory Project*; University of Florida: Integral packages included are VMOL (Almlöf, J.; Taylor, P.R.), BPROPS (Taylor, P.R.), and ABACUS (Helgaker, T.; Jensen, H.J.Aa.; Jorgensen, P.; Olsen, J.; Taylor, P.R.)
- (27) Levine, I. N. *Quantum Chemistry*, 3<sup>rd</sup> ed.; Allyn and Bacon: Boston, 1983:p 373.
- (28) The B3LYP functional uses a three-parameter exchange functional of Becke (B3) [Becke, A.D. *J. Chem. Phys.* **1993**, *98*, 5648; Stephens, P.J.; Devlin, C.F.; Chabalowski, C.F.; Frisch, M.J. *J. Phys. Chem.* **1994**, *98*, 11623] and the Lee, Yang, and Parr (LYP) correlation gradient-corrected functional [Lee, C.; Yang, W.; Parr, R.G. *Phys. Rev. B* **1988**, *37*, 785].
- (29) a) Pople, J.A.; Binkley, J.S.; Seeger, R. *Int. Quantum Chem.* **1976**, *10*, 1.  
 b) Bartlett, R.J.; Silver, D.M. *Int. Quantum Chem.* **1975**, *9*, 183.  
 c) Dupuis, M.; Chin, S.; Marquez, A. in: G. Malli (ed.), *Relativistic and Electron Correlation Effects in Molecules*, Plenum, New York, 1994.  
 d) Frisch, M.J.; Head-Gordon, M.; Pople, J.A. *Chem. Phys. Lett.* **1990**, *166*, 275.  
 e) Bartlett, R.J.; Stanton, R.J. Applications of post-Hartree-Fock methods: A Tutorial, in: Lipkowitz, K.B.; Boyd, D.B. (Eds.), *Reviews of Computational Chemistry*, Vol. V, VCH Publishers, New York, 1994.
- (30) Purvis, G.D., III; Bartlett, R.J. *J. Chem. Phys.* **1982**, *76*, 1910.
- (31) Raghavachari, K.; Trucks, G.W.; Pople, J.A.; Head-Gordon, M. *Chem. Phys. Lett.* **1989**, *157*, 479.
- (32) Roesky, H. W.; Schmieder, W.; Isenberg, W.; Boehler, D.; Sheldrick, G. M. *Angew. Chem., Int. Ed. Engl.* **1982**, *21*, 153; Roesky, H. W.; Panday, K. P.; Krebs, B.; Dartmann, M. *J. Chem. Soc., Dalton Trans.* **1984**, 2271.

- (33) Chivers, T.; Schmidt, K. J.; McIntyre, D. D.; Vogel, H. J. *Can. J. Chem.* **1989**, *67*, 1788.
- (34) Morgon, N. H.; Linnert, H. V.; Riveros, J. M. *J. Phys. Chem.* **1995**, *99*, 11667.
- (35) Seel, F.; Mueller, E. *Chem. Ber.* **1955**, *88*, 1747.
- (36) Christe, K. O.; Dixon, D. A.; McLemore, D.; Wilson, W. W.; Sheehy, J. A.; Boatz, J. A. *J. Fluorine Chem.* **2000**, *101*, 151.
- (37) Bondi, A. *J. Phys. Chem.* **1964**, *68*, 441.
- (38) Lindqvist, I. *Acta Crystallogr.* **1957**, *10*, 406.
- (39) Baggio, S. *Acta Crystallogr.* **1971**, *27*, 517.
- (40) Wang, Y.; Chen, I-C. *Acta Crystallogr., Sect. C* **1984**, *40*, 1780.
- (41) Hvoslef, J.; Tracy, M. L.; Nash, C. P. *Acta Crystallogr., Sect. C*, **1986**, *42*, 353.
- (42) Lork, E.; Mews, R.; Viets, D.; Watson, P. G.; Borrmann, T.; Vij, A.; Boatz, J. A.; Christe, K. O. *Inorg. Chem.* **2001**, *40*, 1303.

**Table 1.**  $^{14}\text{N}$  NMR Spectra of Aqueous and  $\text{SO}_2$  Solutions of  $\text{MN}_3$  ( $\text{M} = \text{Na}, \text{Cs}$  or  $\text{N}(\text{CH}_3)_4$ ) and of  $\text{MSO}_2\text{N}_3$  ( $\text{M} = \text{Cs}$  or  $\text{N}(\text{CH}_3)_4$ ) in  $\text{CH}_3\text{NO}_2$ ,  $\text{CH}_3\text{CN}$ , or  $\text{CHF}_3$  Solution

compound (solvent)	chem shift, ppm (line width, Hz)		
	central	terminal nitrogen	area ratio
$\text{NaN}_3$ ( $\text{H}_2\text{O}$ , 20 °C)	-133.5 (18)	-282.2 (60)	1:2
$\text{NaN}_3$ ( $\text{SO}_2$ , 20 °C) <sup>b</sup>	-135.8 weak	not observed	
$\text{CsN}_3$ ( $\text{SO}_2$ , 20 °C)	-133.9 (15)	-201.7 (76)	1:2
( $\text{SO}_2$ , -25 °C)	-134.3 (19)	-200.1 (150)	1:2
( $\text{SO}_2$ , -65 °C)	-134.7 (51)	-198.9 (235)	1:2
$\text{CsSO}_2\text{N}_3$ ( $\text{CH}_3\text{NO}_2$ , -22 °C)	-132.5 (16)	-209.9 (155)	1:2
$\text{N}(\text{CH}_3)_4\text{N}_3$ ( $\text{H}_2\text{O}$ , 22 °C) <sup>d</sup>	-133.4 (18)	-281.0 (58)	1:2
$\text{N}(\text{CH}_3)_4\text{N}_3$ ( $\text{SO}_2$ , -65 °C) <sup>d</sup>	-135.0 (35)	-199.8 (200)	1:2
$\text{N}(\text{CH}_3)_4\text{SO}_2\text{N}_3$ ( $\text{CH}_3\text{CN}$ , -40 °C) <sup>a,e</sup>	-132.7 <sup>f</sup>	-205.3 (140)	<sup>f</sup>
$\text{N}(\text{CH}_3)_4\text{SO}_2\text{N}_3$ ( $\text{CHF}_3$ , -90 °C) <sup>b</sup>	-136.4 weak	not observed	
$\text{N}(\text{CH}_3)_4(\text{SO}_2)_2\text{N}_3 \cdot n\text{SO}_2$ ( $\text{CH}_3\text{CN}$ , -40 °C) <sup>a,e</sup>	-133.1 <sup>f</sup>	-203.7 (192)	<sup>f</sup>

<sup>a</sup>Clear colorless solution with faint yellow solid. <sup>b</sup>Low solubility. <sup>c</sup>Pale yellow solution with yellow solid. <sup>d</sup>The sharp resonances due to  $\text{N}(\text{CH}_3)_4^+$  were observed at -139.3 ( $\text{H}_2\text{O}$ ) and -336.9 ppm ( $\text{SO}_2$ ). <sup>e</sup>Resonances due to  $\text{CH}_3\text{CN}$  and  $\text{N}(\text{CH}_3)_4^+$  were observed at -137.7 (~300Hz) and -338 ppm, respectively. <sup>f</sup>Not determined due to overlap with solvent resonance.

**Table 2.** Crystal Data and Structure Refinement for  $\text{CsSO}_2\text{N}_3 \cdot \text{CsSO}_2\text{N}_3$  (1)

---

empirical formula	Cs <sub>2</sub> N <sub>6</sub> O <sub>5</sub> S <sub>2</sub>
fw	494.00
Temperature (K)	173(2)
space group	<i>P2<sub>1</sub>/m</i>
<i>a</i> , Å	9.542(2)
<i>b</i> , Å	6.2189(14)
<i>c</i> , Å	10.342(2)
<i>β</i> , deg	114.958(4)
<i>V</i> , Å <sup>3</sup>	556.4(2)
<i>Z</i>	2
$\rho_{\text{calc}}$ g/cm <sup>3</sup>	2.949
$\mu$ , mm <sup>-1</sup>	6.939
crystal size, mm	0.10 x 0.27 x 0.52
$\lambda$ , Å	0.71073
<i>R</i> <sub>int</sub>	0.0446
transmission factors	0.5437- 0.1230
goodness-of-fit on <i>F</i>	1.075
<i>R</i> 1, <i>wR</i> 2 [ <i>I</i> >2σ( <i>I</i> )]	0.0398, 0.1068
<i>R</i> 1, <i>wR</i> 2 (all data)	0.0416, 0.1085

**Table 3. Atomic Coordinates ( $\times 10^4$ ) and Equivalent Isotropic Displacement Parameters ( $\text{\AA}^2 \times 10^3$ ) for  $\text{CsSO}_2\text{N}_3\cdot\text{CsSO}_3\text{N}_3$ .  $U(\text{eq})$  is Defined as one Third of the Trace of the Orthogonalized  $U_{ij}$  Tensor.**

	x	y	z	$U(\text{eq})$
Cs(1)	6199(1)	2500	3672(1)	38(1)
Cs(2)	10539(1)	2500	1983(1)	39(1)
S(1)	6914(2)	2500	7536(2)	42(1)
S(2)	9094(3)	-2500	3854(2)	40(1)
O(1)	8336(7)	2500	8827(6)	59(2)
O(2)	6625(5)	562(8)	6701(5)	49(1)
O(3)	8278(16)	-3010(20)	4683(12)	47(5)
O(4)	8677(11)	-276(12)	3266(9)	45(2)
O(5)	10543(17)	-3070(30)	3910(30)	45(7)
N(1)	5404(10)	1975(19)	8035(10)	49(4)
N(2)	5694(7)	2500	9245(6)	31(1)
N(3)	5843(12)	3101(19)	10317(11)	51(4)
N(4)	7990(17)	-4208(17)	2097(14)	55(3)
N(5)	7791(13)	-3134(14)	1059(12)	40(2)
N(6)	7645(14)	-2130(30)	100(13)	52(5)





Table 4. Most Important Bond Lengths [Å] and Angles [°] of the  $\text{SO}_2\text{N}_3^-$  Anion in its  $\text{Cs}^+$  Salt Compared to Those in  $[\text{N}(\text{CH}_3)_4]^+\text{SO}_2\text{N}_3^-$  and the Calculated<sup>a</sup> Values

	calculated				observed	
	RHF	B3LYP	MP2	CCSD(T)	$\text{Cs}^+\text{SO}_2\text{N}_3^-$	$[\text{N}(\text{CH}_3)_4]^+\text{SO}_2\text{N}_3^-^b$
<b>bond distances (Å)</b>						
S-N	1.907	2.226	2.356	2.198	1.981(12)	2.005(2)
S-O <sup>c</sup>	1.464	1.492	1.492	1.494	1.410(10) <sup>e</sup>	1.453(2)
S-O <sup>d</sup>	1.462	1.490	1.491	1.493	1.495(8)	1.457(2)
N $\alpha$ -N $\beta$	1.205	1.207	1.223	1.222	1.209(16)	1.214(2)
N $\beta$ -N $\gamma$	1.113	1.169	1.205	1.182	1.130(16)	1.144(2)
<b>bond angles (°)</b>						
O-S-N <sup>d</sup>	101.46	99.21	99.94	99.01	100.1(5)	96.82(8)
O-S-N <sup>e</sup>	102.09	102.42	102.24	101.46	102.7(11) <sup>f</sup>	100.87(9)
S-N $\alpha$ -N $\beta$	112.0	110.29	106.81	108.67	110.0(8)	110.22(14)
N $\alpha$ -N $\beta$ -N $\gamma$	178.9	179.16	179.32	179.37	178.2(15)	178.6(2)
O-S-O	112.6	114.58	115.58	114.90	111.1(9) <sup>g</sup>	112.72(10)

<sup>a</sup>A 6-31+G(d) basis set was used for all calculations. <sup>b</sup>Data from ref 2. <sup>c</sup>Oxygen atom that is approximately perpendicular to the plane of the  $\text{N}_3\text{S}$  fragment. <sup>d</sup>Oxygen atom that is approximately in plane with the  $\text{N}_3\text{S}$  fragment. <sup>e</sup>Average value from disordered positions. <sup>f</sup>Taken from the major component of the disordered oxygen position.

**Table 5. Most Important Bond Lengths [Å] and Angles [°] of the  $\text{SO}_3\text{N}_3^-$  Anion in its  $\text{Cs}^+$  Salt Compared to the Calculated<sup>a</sup> Values**

	calculated		observed
	B3LYP /6-31+G(d)	MP2 /6-31+G(d)	
<b>bond distances (Å)</b>			
S-N	1.876	1.871	1.754(10)
S-O'	1.473	1.472	1.440(5)
S-O <sub>2</sub>	1.479	1.478	1.447(6)
N $\alpha$ -N $\beta$	1.223	1.233	1.207(11)
N $\beta$ -N $\gamma$	1.151	1.175	1.120(11)
<b>bond angles (°)</b>			
O'-S-N	99.59	99.31	92.7(4)
O <sub>2</sub> -S-N	102.94	102.47	107.2(4)
S-N $\alpha$ -N $\beta$	114.21	114.52	110.0(8)
N $\alpha$ -N $\beta$ -N $\gamma$	175.39	174.48	173.5(10)
O'-S-O <sub>2</sub>	116.18	116.45	114.9(2)
S-N-N-N	180.00	180.00	180.0
O'-S-N-N	180.00	180.00	180.0



Table 6. continued....

vibrational frequencies, cm <sup>-1</sup>					assignments		
RHF	calcd for free SO <sub>2</sub> N <sub>3</sub> <sup>-</sup>			exp	SO <sub>2</sub> N <sub>3</sub> <sup>-</sup>	N(CH <sub>3</sub> ) <sub>4</sub> <sup>+</sup>	
	MP2	B3LYP	CCSD(T)				
793(10)[10]	586(1)[4]	646(6)[1]	598	662mw	660(3)	663(2)	δ(N <sub>3</sub> ) in SN <sub>3</sub> plane
700(18)[0.1]	550(1)[1]	608(6)[3]	549				δ(N <sub>3</sub> ) out of SN <sub>3</sub> plane
607(116)[1.4]	497(33)[4]	504(27)[4]	505	547m	540(7)	543(5)	δ <sub>sciss</sub> (SO <sub>2</sub> )
499(263)[6.4]	329(133)[10]	369(122)[8]	368	414ms	420(15)	428(17)	ν <sub>19</sub> (F <sub>2</sub> ), δ(CN <sub>4</sub> )
352(13)[2.9]	181(11)[12]	220(1)[6]	223				ν <sub>12</sub> (F <sub>1</sub> ), τ(CH <sub>3</sub> )
310(189)[29]	167(38)[17]	181(50)[20]	177		309(30)	317(45)	τ(SO <sub>2</sub> )
150(4.0)[11]	69(4)[11]	106(9)[14]	96		258(84)	269(100)	ν(SN)
					169(20)	175(24)	δ <sub>sciss</sub> (SNIN)
						125sh	lattice vibrations
					96(100)	103(56)	
					86sh		
					78(31)		
17(0.9)[8.4]	30(1)[10]	22(1)[7]	25			78(27)	τ(O <sub>2</sub> S-N <sub>3</sub> )

<sup>a</sup>Bands arising from the FEP sample tube were observed at 735 (2) cm<sup>-1</sup> in the spectrum of the N(CH<sub>3</sub>)<sub>4</sub><sup>+</sup> salt.

Table 7. Vibrational Spectra of  $[N(CH_3)_4]([SO_2)_2N_3]$  and  $[Cs]([SO_2)_2N_3]$  and Assignments for  $(SO_2)_2N_3$  Based on the Frequencies and Intensities Calculated at the MP2 and B3LYP Levels of Theory.<sup>a,b</sup>

vibrational frequencies, $cm^{-1}$				assignments	
$O_2SNNNSO_2$		calcd for free $(O_2S)_2NNN$		exp	$(O_2S)_2N_3N(CH_3)_4^+$
MP2	B3LYP	B3LYP	MP2		
				$N(CH_3)_4^+Cs^+$ Raman, -80 °C	
				Raman, -100 °C	
				3052(8)sh	v(CH <sub>3</sub> ) modes
				3043(12)	
				3037(8)sh	
				2992(13)	
				2976(5)	
				2960(6)	
				2930(10)	
				2903(1)	
				2826(4)	v <sub>s</sub> (N <sub>3</sub> )
2096(10)[93]	2076(35)[11]	2125(21)[137]	2102(12)[206]	2028(1)	
				1981(13)	
				1492(1)	
				1471(1)	
				1455(6)	
				1422(1)	
				1383(1)	
				1333(13)	v <sub>i</sub> (N <sub>3</sub> )
1241(0)[46]	1379(0)[22]	1339(2)[11]	1252(4)[58]	1316(2)	
				1299(5)	
1236(1)[67]	1243(11)[29]	1235(5)[24]	1242(5)[38]	1273(5)	
1228(8)[13]	1241(0)[17]	1224(5)[24]	1217(0.1)[32]	1246(2)	
				1223(3)	
				1177(1)	
				1140(100)	
				1136(98)	v <sub>i</sub> (SO <sub>2</sub> )
1052(1)[457]	1094(4)[307]	1088(2)[176]	1080(4)[287]	1120(100)	
1052(5)[143]	1077(7)[112]	1078(6)[51]	1067(2)[219]	1113(6)	
				1099(41)	
				1096sh	
				1082(1)	

Table 7. continued...

vibrational frequencies, cm <sup>-1</sup>				assignments	
calcd for free (O <sub>2</sub> S) <sub>2</sub> NNN <sup>+</sup>				(O <sub>2</sub> S) <sub>2</sub> N <sub>2</sub> N(CH <sub>3</sub> ) <sub>4</sub> <sup>+</sup>	
				exp	
O <sub>2</sub> SNNNSO <sub>2</sub> <sup>-</sup>					
MP2	B3LYP	B3LYP	MP2	N(CH <sub>3</sub> ) <sub>4</sub> <sup>+</sup> Cs <sup>+</sup> Raman, -80 °C <sup>a</sup>	Raman, -100 °C
563(0)[2]	640(0)[4]	638(0)[2]	563(0.1)[0.6]	1074(1)	v <sub>18</sub> (F <sub>2</sub> ), v <sub>16</sub> (CN <sub>4</sub> ) v <sub>3</sub> (A <sub>2</sub> ), v <sub>1</sub> (CN <sub>4</sub> )
546(0)[1]	620(0)[1]	606(0)[2]	502(0.3)[1.4]	956(4)	
				756(6)	
488(1)[0]	501(1)[11]	504(1)[2]	491(0.1)[5]	536(4)	δ <sub>as</sub> (SO <sub>2</sub> )
487(0)[5]	498(0)[0]	503(0)[5]	487(1)[5]	458(2)	
				384(1)	
276(2)[8]	306(0)[15]	323(2)[6]	312(2)[5]	370(1)	v <sub>19</sub> (F <sub>2</sub> ), δ(CN <sub>4</sub> ) v <sub>12</sub> (F <sub>1</sub> ), τ(CH <sub>3</sub> )
261(1)[5]	281(5)[1]	308(4)[4]	276(3)[15]	292(1)	
201(0)[10]	209(0)[16]	247(1)[3]	221(1)[9]	231(7)	
201(0)[15]	172(0)[3]	181(0)[8]	162(0.4)[2]	206(5)	352(2)
140(0)[5]	131(0)[10]	146(1)[4]	139(0.4)[7]	183(4)	
135(1)[0]	130(2)[1]	112(0)[15]	109(0.1)[7]	161(14)	
109(0)[1]	71(0)[4]	78(0)[4]	79(0.03)[9]	139(12)	117(5)
97(0)[2]	52(0)[3]	73(0)[6]	68(0.08)[6]	117(5)	
71(0)[5]	20(0)[10]	34(0)[2]	45(0.01)[3]	105(11)	
47(0)[1]	19(0)[1]	30(0)[3]	26(0.05)[2]	89(5)	78(5)
				78(5)	
				69(4)	
34(0)[0]	1(0)[1]	22(0)[0]	23(0.03)[2]	54(4)	

<sup>a</sup> Bands arising from the FEP sample tube were observed at 734 (3) cm<sup>-1</sup> for the N(CH<sub>3</sub>)<sub>4</sub>(O<sub>2</sub>S)<sub>2</sub>N<sub>3</sub> sample. <sup>b</sup> Raman spectra of Cs(O<sub>2</sub>S)<sub>2</sub>N<sub>3</sub> recorded at -130 °C on the Cary instead of the Bruker Equinox showed significant changes in the relative intensities of some of the bands.

Table 8. Vibrational Spectra of [Cs][SO<sub>3</sub>N<sub>3</sub>]

vibrational frequencies, cm <sup>-1</sup>				assignments
exp		calc		SO <sub>3</sub> N <sub>3</sub> <sup>-</sup> (C <sub>s</sub> )
IR, 22 °C	Raman, 22 °C	MP2	B3LYP	
3337m				2134+1247 ( $\nu_1 + \nu_{11}$ )
2469m				1269+1247 ( $\nu_3 + \nu_{11}$ )
2450m				2x1247 (2x $\nu_{11}$ )
2283w				1247+1045 ( $\nu_4 + \nu_{11}$ )
2134vs	2138(23) 2118(15)	2272(19)[81]	2192(827)[89]	$\nu_1$ (A'), $\nu_{as}$ (N <sub>3</sub> )
1483w				2x744 (2x $\nu_2$ )
	1278(8)	1285(1)[1]	1323(136)[8]	$\nu_2$ (A'), $\nu_s$ (N <sub>3</sub> )
1269vs		1283(9)[16]	1241(318)[14]	$\nu_3$ (A'), $\nu_{as}$ (SO <sub>3</sub> )
1247vs	1250(9)	1261(9)[7]	1218(336)[9]	$\nu_{11}$ (A''), $\nu_{as}$ (SO <sub>3</sub> )
1114w	1089(5)			
1045vs	1052(100)	1022(4)[44]	987(158)[40]	$\nu_4$ (A'), $\nu_s$ (SO <sub>3</sub> )
1028w				562+464 ( $\nu_{13} + \nu_9$ )
744s	746(18)	706(0.5)[5]	700(18)[5]	$\nu_5$ (A'), $\delta$ (N <sub>3</sub> ) in plane
640sh	644(10)	558(0.1)[0.1]	593(8)[0.1]	$\nu_{12}$ (A''), $\delta$ (N <sub>3</sub> ) out of
plane				
626vs		563(9)[7]	572(349)[6]	$\nu_6$ (A'), $\delta$ (SO <sub>3</sub> )
umbrella				
618m				2x313 (2x $\nu_4$ )
579w				
562s	558(13)	519(1)[4]	510(28)[4]	$\nu_{13}$ (A''), $\delta_{as}$ (SO <sub>3</sub> )
556s				
547s	550sh	518(0.5)[3]	509(18)[3]	$\nu_7$ (A'), $\delta_{aciss}$ (SO <sub>2</sub> )
464m	464(54)	363(2)[29]	369(34)[24]	$\nu_9$ (A'), $\nu$ (S-N)
	370(28)	314(1)[11]	314(11)[9]	$\nu_8$ (A'), $\delta_{rock}$ (SO <sub>3</sub> )
	364sh			
	313(8)	322(0)[1]	318(0)[1]	$\nu_{14}$ (A''), $\delta_{wag}$ (SO <sub>3</sub> )
	185(23)	123(0)[7]	139(1)[6]	$\nu_{10}$ (A'), $\delta_{aciss}$ (S-N-N)
	112sh			
		49(0)[6]	33(0)[6]	$\nu_{15}$ (A''), $\tau$ (S-N)



## Diagram Captions

Figure 1. Crystal Structure of  $\text{CsSO}_2\text{N}_3\cdot\text{CsSO}_3\text{N}_3$ .

Figure 2. A 30% Ortep plot of the experimental  $\text{SO}_2\text{N}_3^-$  structure.

Figure 3. Structure of the  $\text{SO}_2\text{N}_3^-$  anion calculated at the CCSD(T)/6-31+G(d) level.

Figure 4. Crystal structure of the  $\text{SO}_3\text{N}_3^-$  anion in its Cs salt, showing the disorder of N1 and N3 across the crystallographic mirror plane.

Figure 5. A 30% Ortep plot of the experimental  $\text{SO}_3\text{N}_3^-$  structure.

Figure 6. Structure of the  $\text{SO}_3\text{N}_3^-$  anion calculated at the MP2/6-31+G(d) level.

Figure 7. Packing diagram of  $\text{CsSO}_2\text{N}_3\cdot\text{CsSO}_3\text{N}_3$  showing the cesium-sulfur network.

Figure 8. Raman spectrum of  $\text{CsSO}_2\text{N}_3$ .

Figure 9. Raman spectrum of  $\text{N}(\text{CH}_3)_4\text{SO}_2\text{N}_3$ .

Figure 10. Raman spectrum of  $\text{Cs}(\text{SO}_2)_2\text{N}_3$ .

Figure 11. Infrared (upper trace) and Raman (lower trace) spectra of  $\text{CsSO}_3\text{N}_3$ .

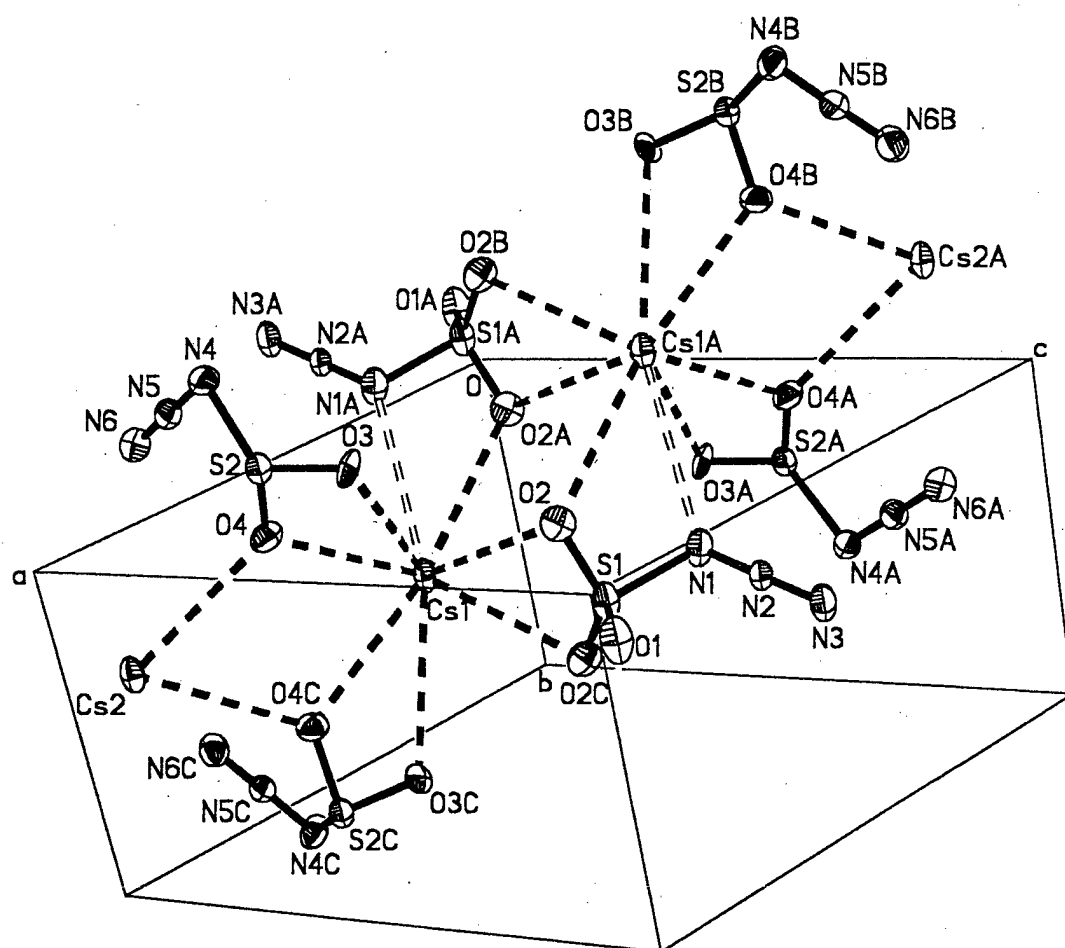
Figure 12. Structure of the  $\text{SO}_2\text{N}_3^-$  anion calculated at the RHF/6-31+G(d) level.

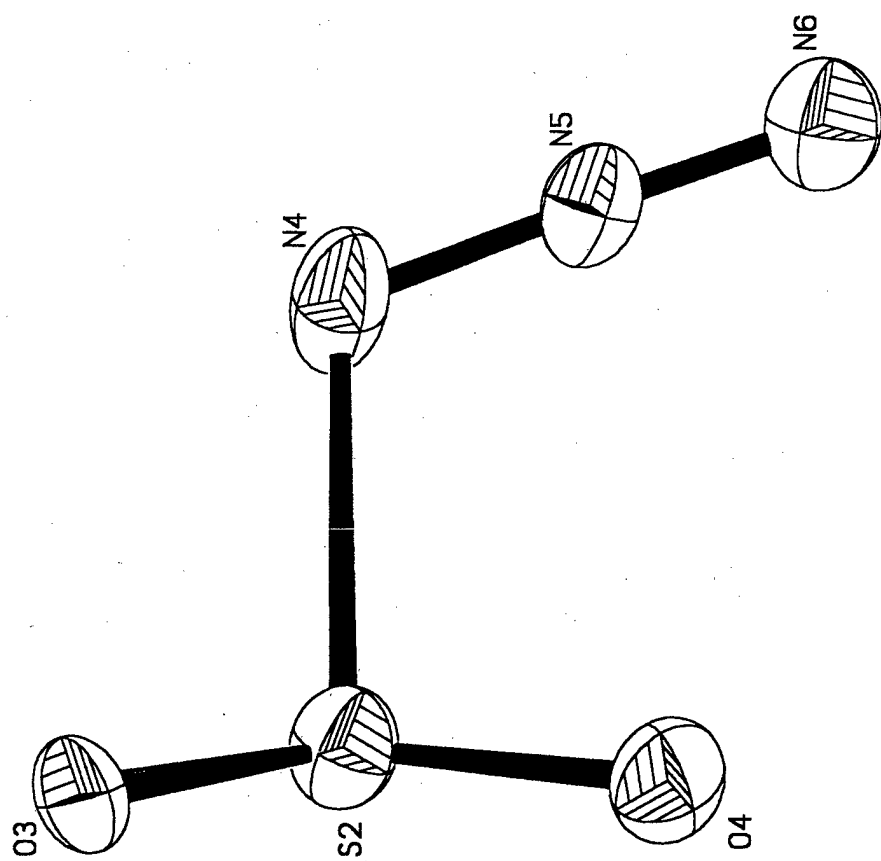
Figure 13. Structure of the  $1,3-(\text{SO}_2)_2\text{N}_3^-$  anion calculated at the B3LYP/6-31+G(d) level.

Figure 14. Structure of the  $1,3-(\text{SO}_2)_2\text{N}_3^-$  anion calculated at the MP2/6-31+G(d) level.

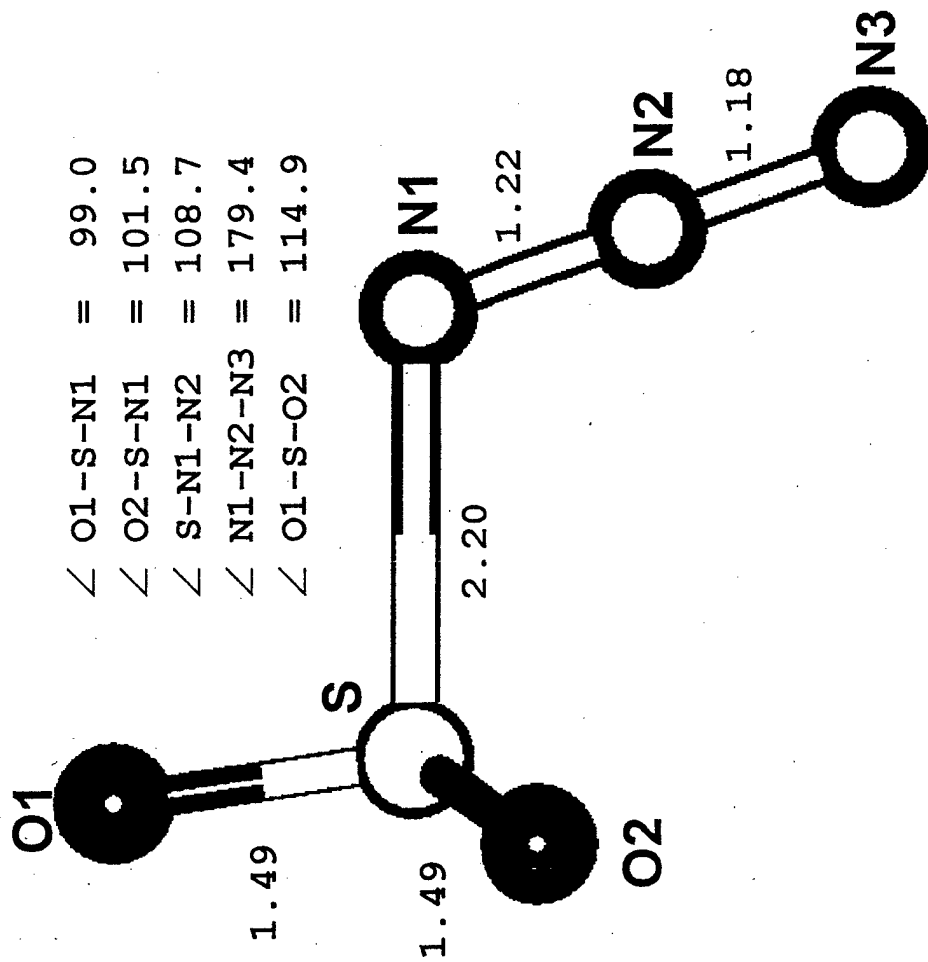
Figure 15. Structure of the  $1,1-(\text{SO}_2)_2\text{N}_3^-$  anion calculated at the B3LYP/6-31+G(d) level.

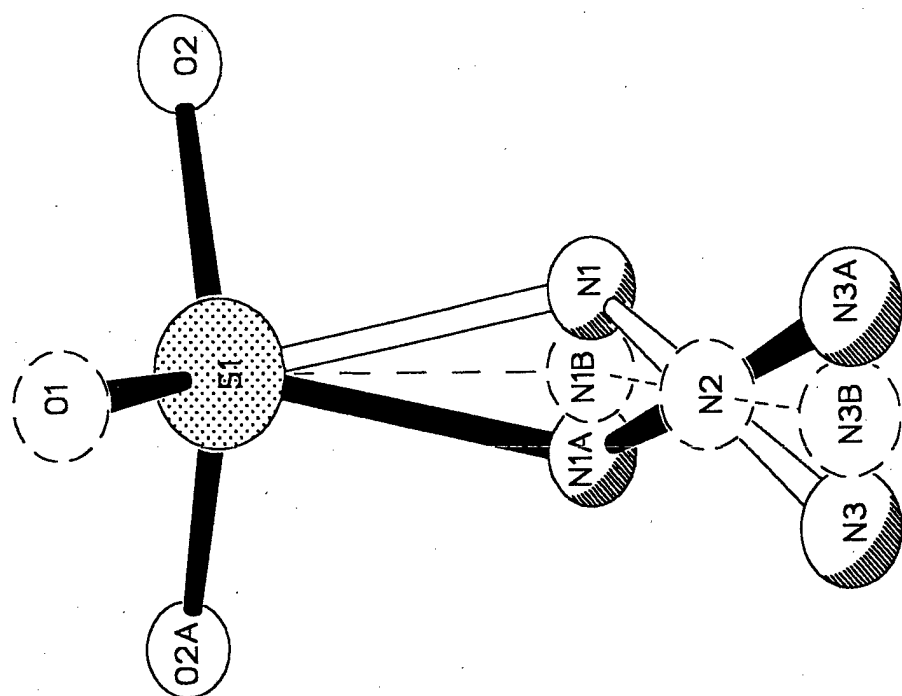
Figure 16. Structure of the  $1,1-(\text{SO}_2)_2\text{N}_3^-$  anion calculated at the MP2/6-31+G(d) level.

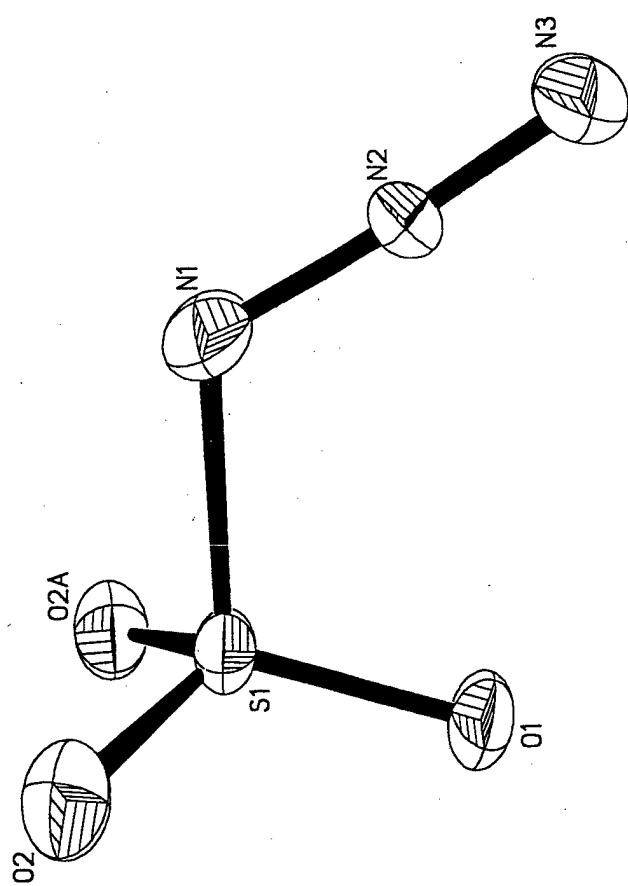




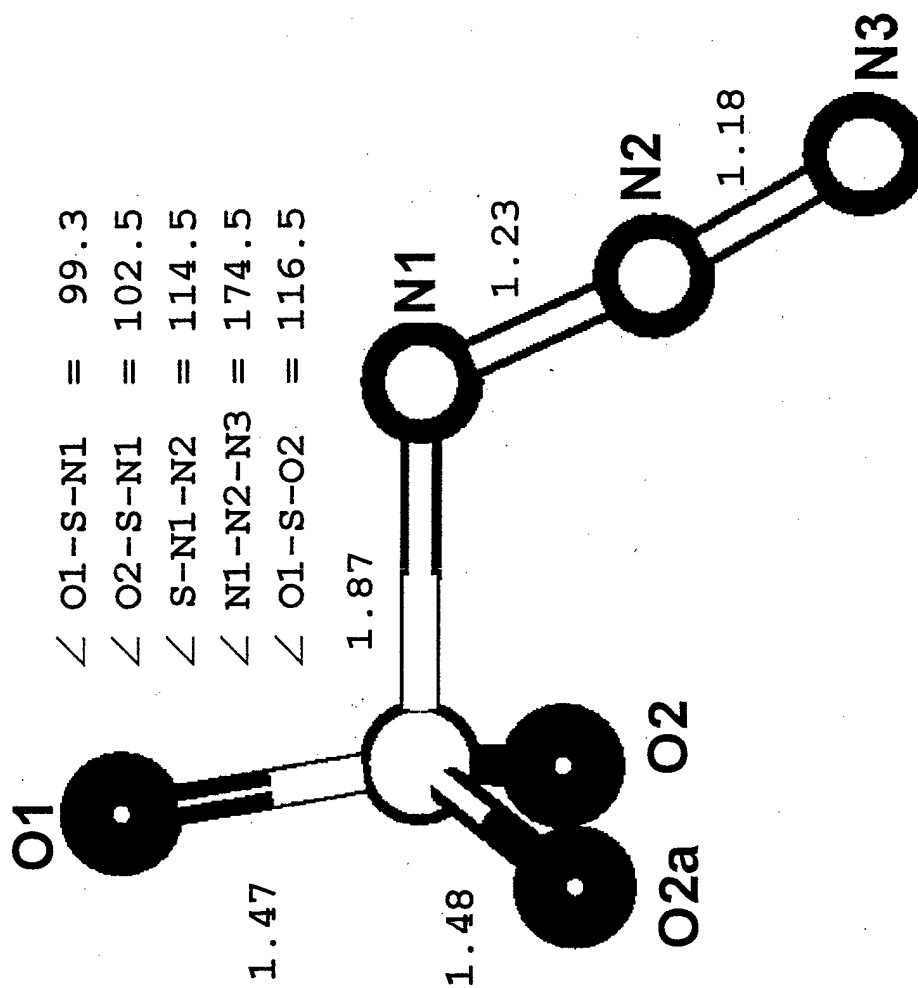
CCSD (T) / 6-31+G (d)

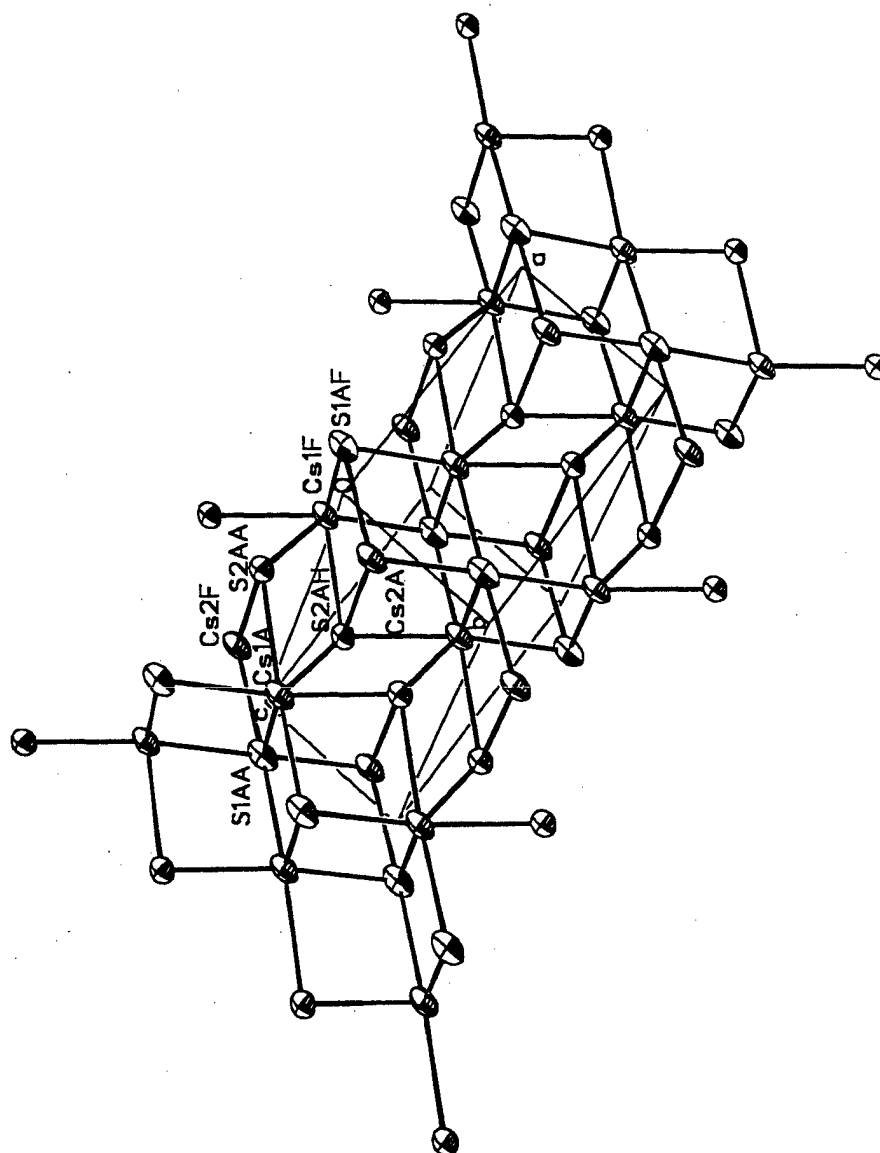




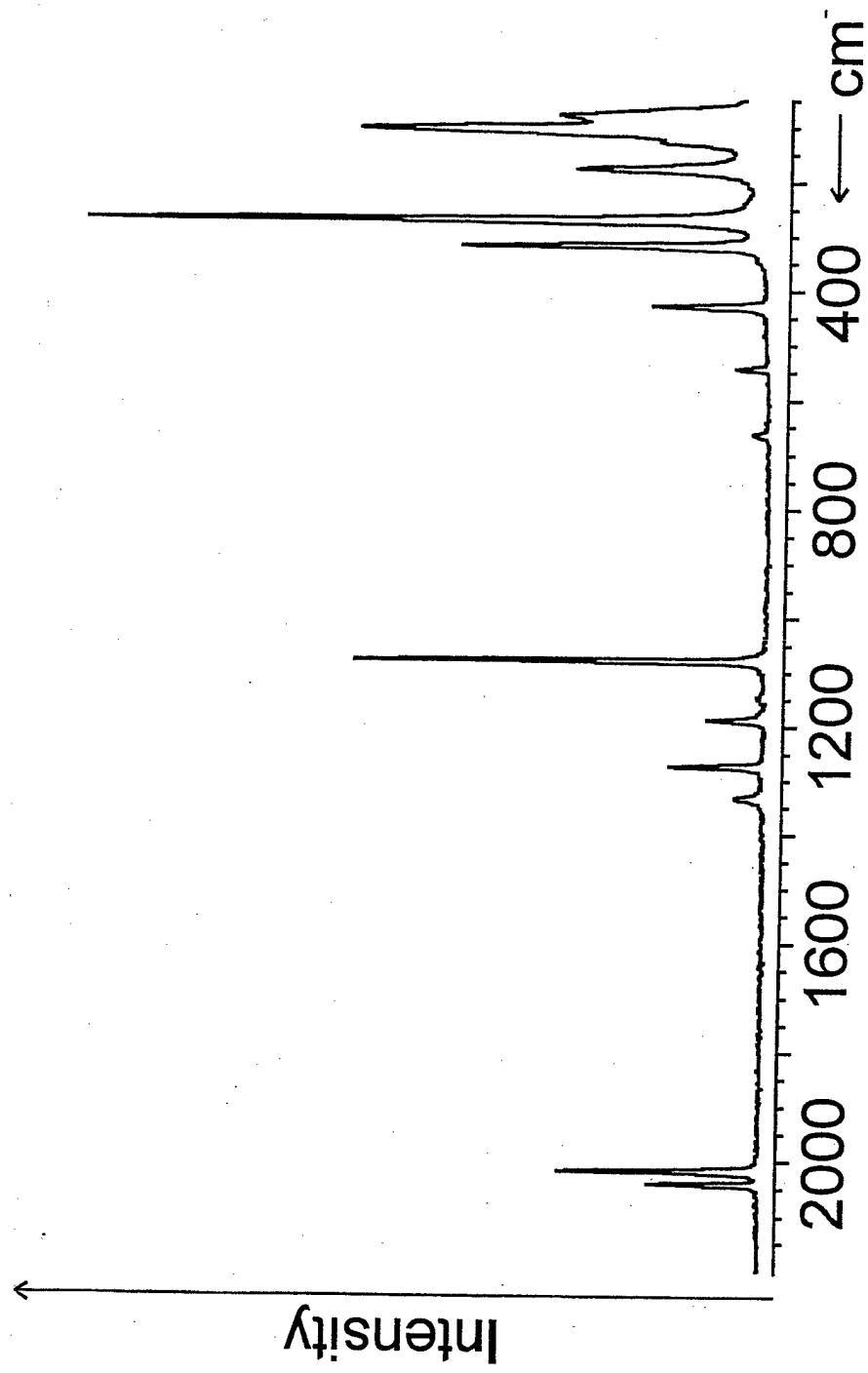


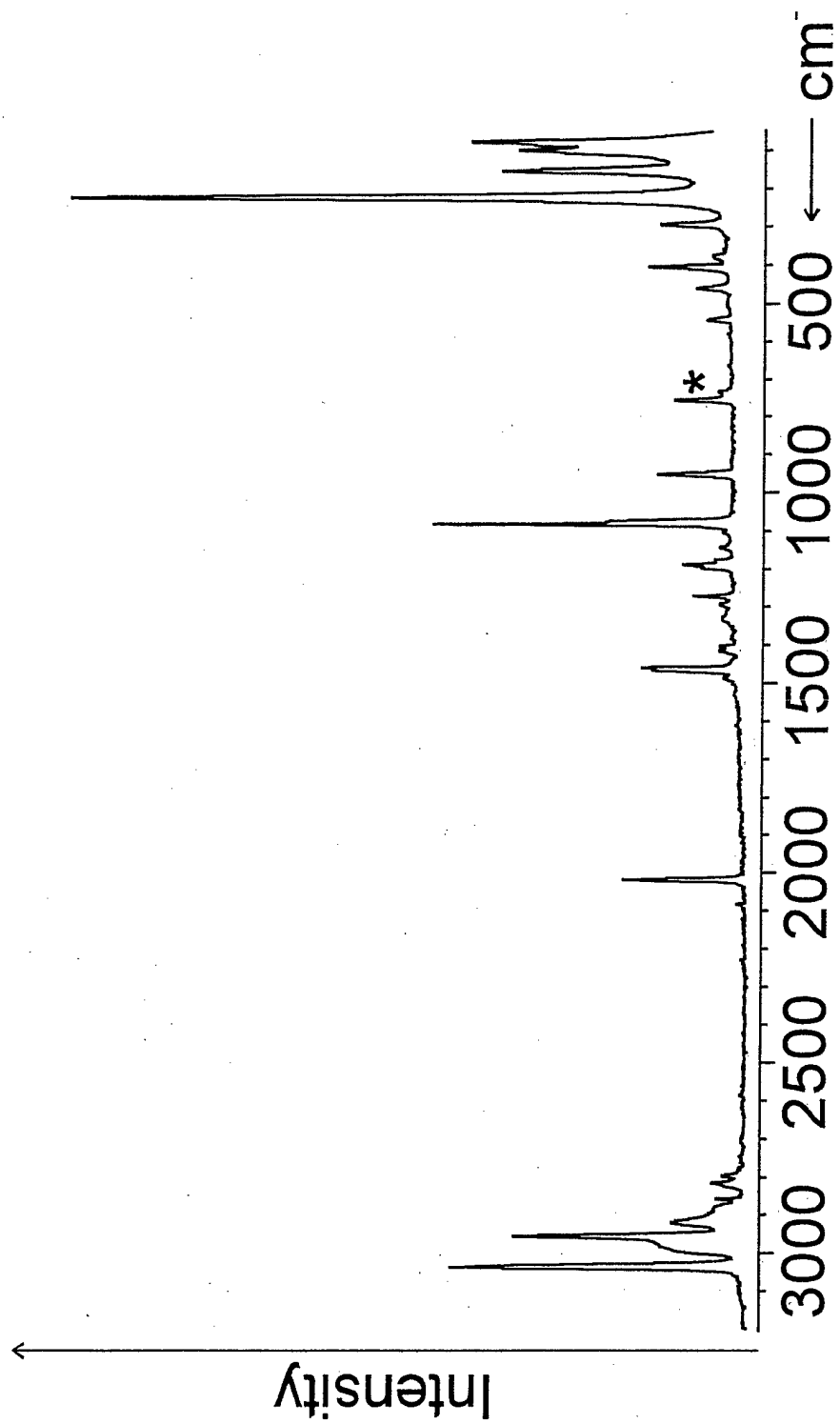
MP2/6-31+G(d)

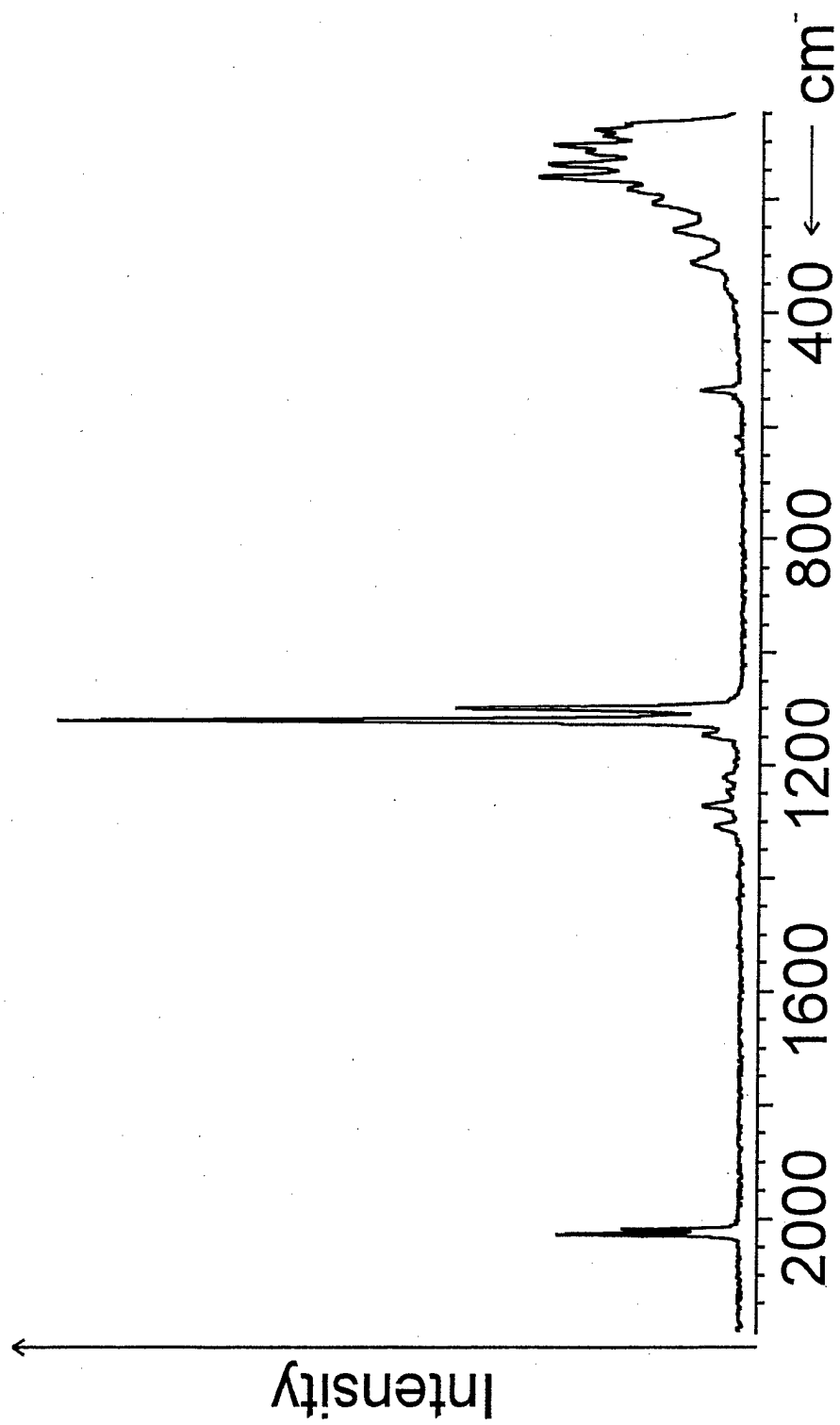


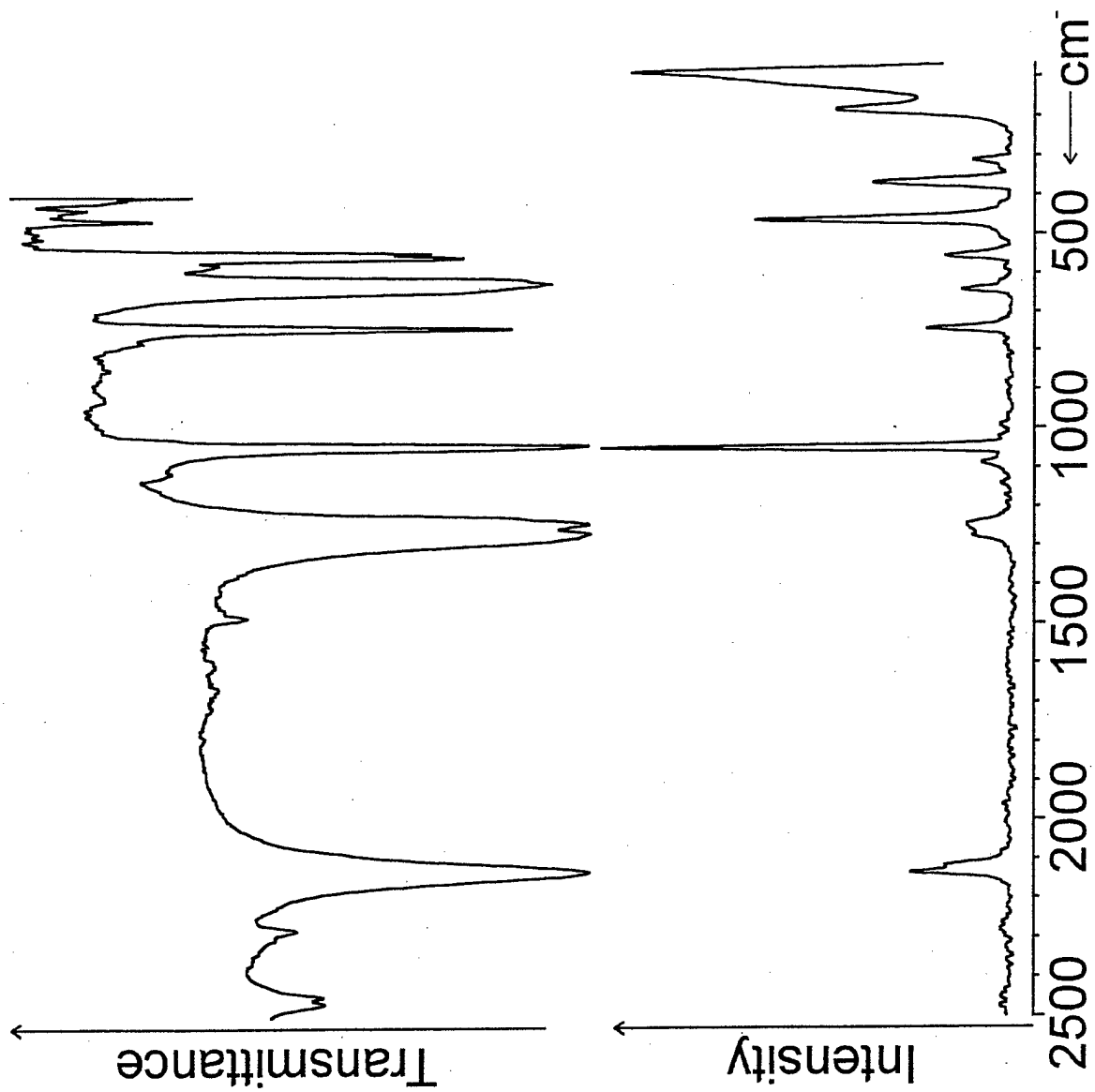




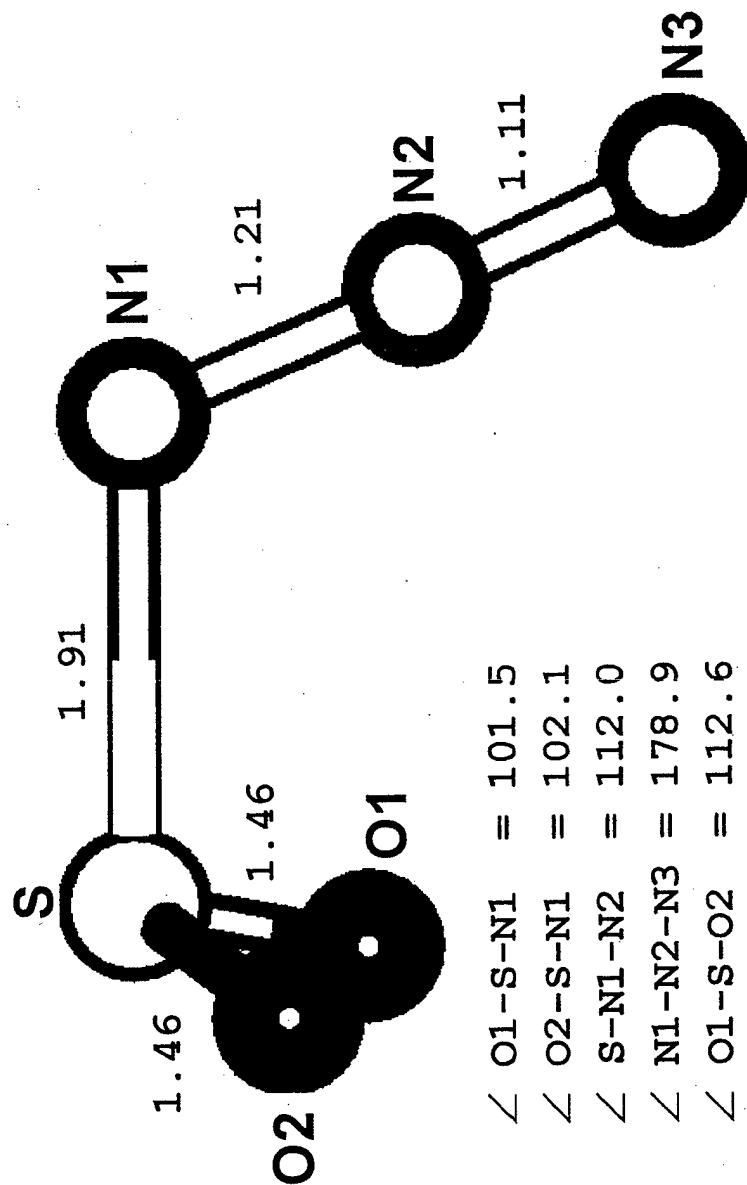




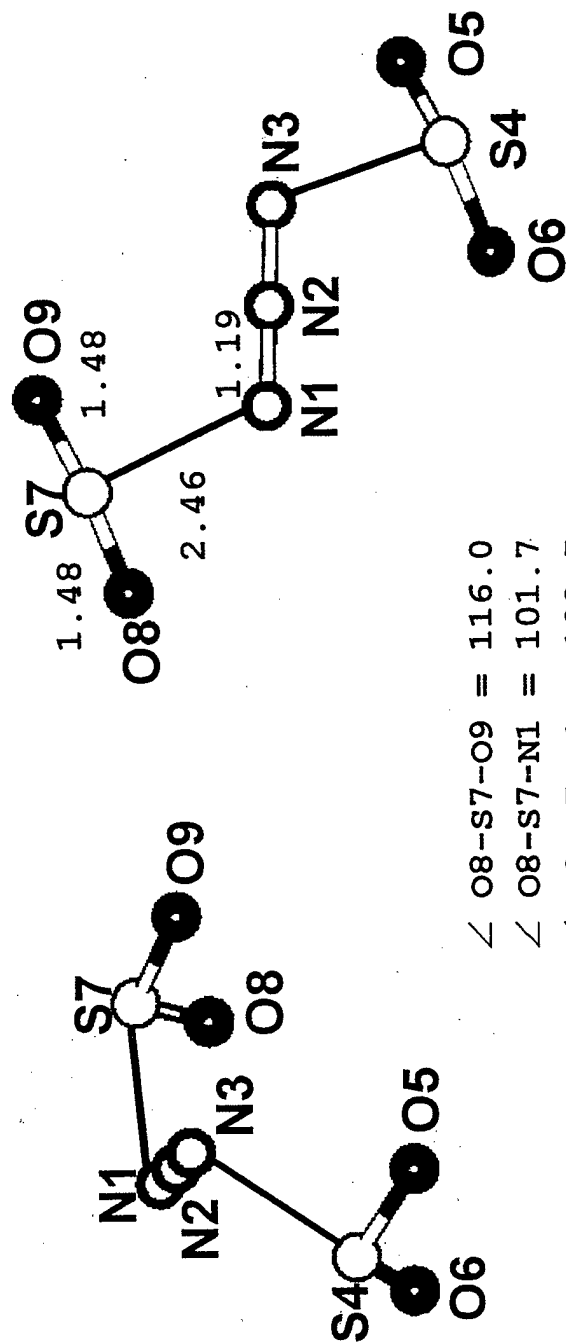




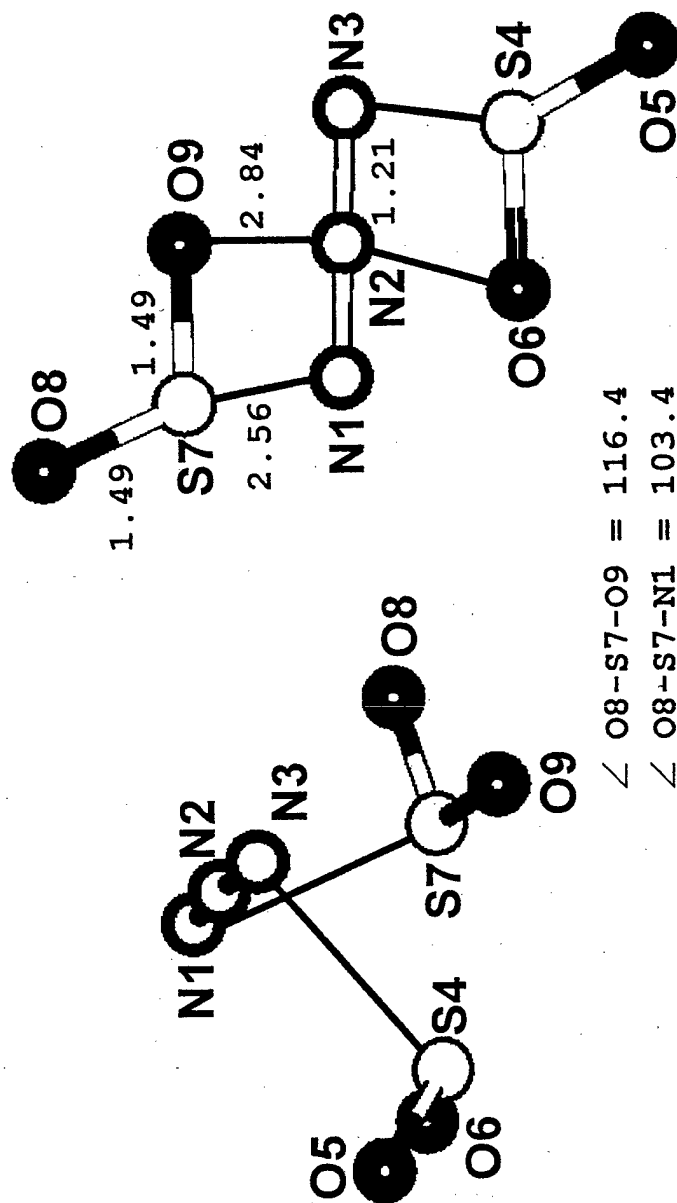
RHF/6-31+G(d)



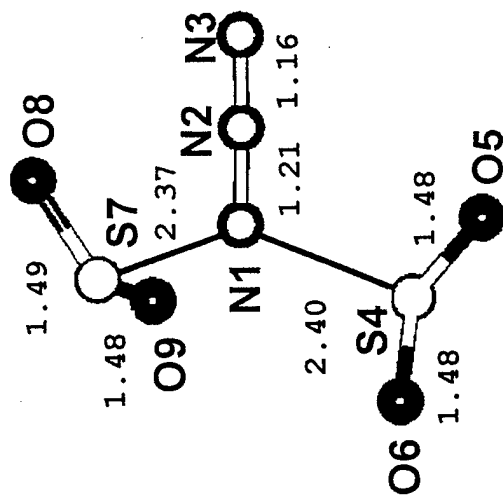
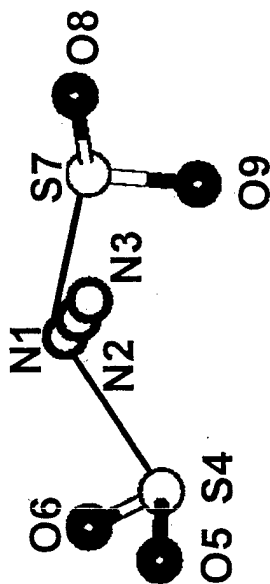
B3LYP/6-31+G(d)



$\angle$  O8-S7-O9 = 116.0  
 $\angle$  O8-S7-N1 = 101.7  
 $\angle$  O9-S7-N1 = 102.5  
 $\angle$  S7-N1-N2 = 111.9  
 $\angle$  N1-N2-N3 = 179.2  
 $\omega$  O8-S7-N1-N2 = 134.1  
 $\omega$  O9-S7-N1-N2 = 13.9  
 $\omega$  S7-N1-N3-S4 = -130.0



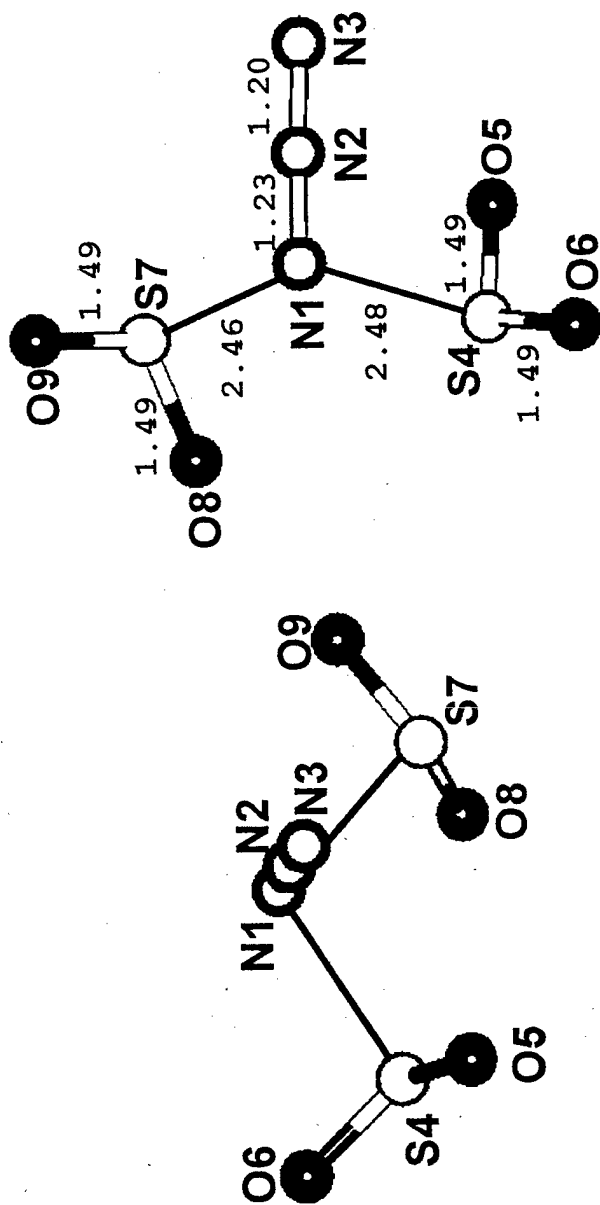
$\angle$ O8-S7-O9 =	116.4
$\angle$ O8-S7-N1 =	103.4
$\angle$ O9-S7-N1 =	97.1
$\angle$ S7-N1-N2 =	93.6
$\angle$ N1-N2-N3 =	174.7
$\omega$ O8-S7-N1-N2 =	-114.8
$\omega$ O9-S7-N1-N2 =	4.6
$\omega$ S7-N1-N3-S4 =	-71.7



$\angle$  O8-S7-O9 = 115.2  
 $\angle$  O8-S7-N1 = 99.7  
 $\angle$  O9-S7-N1 = 102.2  
 $\angle$  S7-N1-N2 = 108.7  
 $\angle$  S4-N1-S7 = 117.5  
 $\omega$  O8-S7-N1-N2 = -18.6  
 $\omega$  O9-S7-N1-N2 = 100.0

$\angle$  O5-S4-O6 = 115.5  
 $\angle$  O5-S4-N1 = 98.9  
 $\angle$  O6-S4-N1 = 100.8  
 $\angle$  S4-N1-N2 = 112.9  
 $\angle$  N1-N2-N3 = 178.9  
 $\omega$  O5-S4-N1-N2 = 32.0  
 $\omega$  O6-S4-N1-N2 = 150.3





$\angle$ O8-S7-O9 = 116.3	$\angle$ O5-S4-O6 = 116.3
$\angle$ O8-S7-N1 = 100.3	$\angle$ O5-S4-N1 = 97.3
$\angle$ O9-S7-N1 = 101.2	$\angle$ O6-S4-N1 = 102.1
$\angle$ S7-N1-N2 = 102.3	$\angle$ S4-N1-N2 = 99.3
$\angle$ S4-N1-S7 = 100.7	$\angle$ N1-N2-N3 = 177.5
$\omega$ O8-S7-N1-N2 = 147.3	$\omega$ O5-S4-N1-N2 = -19.5
$\omega$ O9-S7-N1-N2 = -93.1	$\omega$ O6-S4-N1-N2 = 99.5

Karl O. Christe,<sup>\*†</sup> Jerry A. Boatz,<sup>†</sup> Michael Gerken,<sup>\* Ralf Haiges,<sup>\* Stefan Schneider,<sup>\* Thorsten Schroer,<sup>\* Fook S. Tham,<sup>† Ashwani Vij,<sup>† Vandana Vij,<sup>†</sup> Ross L. Wagner,<sup>\* and William W. Wilson<sup>†</sup></sup></sup></sup></sup></sup></sup></sup>

*Inorg. Chem.* 2002, 41, ...

Synthesis and Characterization of the  $\text{SO}_3\text{N}_3^-$ ,  $(\text{SO}_3)_2\text{N}_3^-$ , and  $\text{SO}_3\text{N}_3^-$  Anions

The azide anion forms colorless 1:1 and yellow 1:2 adducts with  $\text{SO}_3$ . These adducts were characterized by vibrational and NMR spectroscopy and theoretical calculations. The crystal structure of  $\text{CsSO}_3\text{N}_3\cdot\text{CsSO}_3\text{N}_3$  was determined and shows that the N-S bond in  $\text{SO}_3\text{N}_3^-$  is .23 Å longer than that in  $\text{SO}_3\text{N}_3^-$ . Both N-S bonds are unusually long, resulting in facile  $\text{SO}_3$  ligand exchange and low barriers toward rotational disorder.

